UNIVERSITY OF HAWAII
APR 4 '56

GEOCHIMICA ET COSMOCHIMICA ACTA

EDITORIAL ADVISORY BOARD

L. H. AHRENS-OXFORD · T. BARTH-OSLO · N. L. BOWEN-WASHINGTON, D.C. · A. F. BUDDINGTON-PRINCETON, N.J. · L. CAPDECOMME-TOULOUSE · E. J. CONWAY-DUBLIN · P. ESKOLA-HELSINKI · P. GALLITELLI-MODENA · J. GOGUEL-PARIS · D. GUIMARÃES-BELO HORIZONTE · A. HADDING-LUND · O. HAHN-GÖTTINGEN · H. W. HARVEY-PLYMOUTH · F. HEIDE-JENA · A. HOLMES-EDINBURGH · G. E. HUTCHINSON-NEW HAVEN, CONN. · W. Q. KENNEDY-LEEDS · PH. H. KUENEN-GRONINGEN · S. LANDERGREN-STOCKHOLM · F. MACHATSCHKI-VIENNA · B. H. MASON-BLOOMINGTON, IND. · A. MUIR-HARPENDEN · J. ORCEL-PARIS · K. RANKAMA-HELSINKI · E. REINHARD-BASLE · TH. G. SAHAMA-HELSINKI · C. E. TILLEY-CAMBRIDGE · H. C. UREY CHICAGO · T. VOGT-TRONDHEIM · W. WAHL-HELSINKI · T. WATANABE-TOKYO · F. WHIPPLE-CAMBRIDGE, MASS. · R. WILDT-NEW HAVEN, CONN.

EDITORS

C. W. CORRENS, GÖTTINGEN
E. INGERSON, WASHINGTON
S. R. NOCKOLDS, CAMBRIDGE
F. A. PANETH, MAINZ
L. R. WAGER, OXFORD
F. E. WICKMAN, STOCKHOLM

VOLUME 5 No. 6

JUNE, 1954

PERGAMON PRESS LTD · LONDON

Geochim. et Cosmochim. Acta
QE351
.G25

GEOCHIMICA ET COSMOCHIMICA ACTA

EDITORS

PROF. C. W. CORRENS, *Sedimentpetrographisches Institut der Universität, Lotzestr. 13, Göttingen, British Zone, Germany.*

DR. E. INGERSON, *United States Department of the Interior, U.S. Geological Survey, Washington 25, D.C., U.S.A.*

DR. S. R. NOCKOLDS, *Department of Mineralogy and Petrology, The University, Cambridge, England.*

PROF. F. A. PANETH, F.R.S., *Max-Planck-Institut für Chemie, Mainz, Saarstrasse 23, Germany.*

PROF. L. R. WAGER, F.R.S., *Department of Geology and Mineralogy, The University, Oxford, England.*

PROF. F. E. WICKMAN, *Naturhistoriska Riksmuseets, Mineralogiska Avdelning, Stockholm 50, Sweden.*

PERGAMON WAS THE NAME OF A GREEK TOWN IN ASIA MINOR, FAMOUS FOR ONE OF THE GREAT WORKS OF ART, THE ALTAR OF PERGAMON, DEDICATED TO ATHENA.

THE COLOPHON ON THE FRONT COVER IS A REPRODUCTION OF A COIN FOUND AT HERAKLEIA, DATING FROM ABOUT FOUR-HUNDRED B.C., SHOWING THE HEAD OF ATHENA.

VOLUME 5, NO. 6 JUNE 1954

CONTENTS

PAGE

S. R. NOCKOLDS and R. ALLEN: The geochemistry of some igneous rock series: Part II 245

H. G. THODE, R. K. WANLESS and R. WALLOUCH: The origin of native sulphur deposits from isotope fractionation studies 286

Geochemical Note:

KURT SERVOS: Meteorites in the Carl Bosch Collection of Minerals, Yale University. . 299

Publishing Offices: Pergamon Press Ltd., Maxwell House, Marylebone Road, London, N.W.1 (AMB 3421).

Subscription per volume (including postage) £4 10s. (U.S.A. $12.60).

Distributors: Lange, Maxwell & Springer Ltd., Maxwell House, Marylebone Road, London, N.W.1.

and Lange, Maxwell & Springer Inc., 122 East 55th Street, New York 22. N.Y.

PERGAMON PRESS LTD., MAXWELL HOUSE, MARYLEBONE ROAD, LONDON, N.W.1

Geochimica et Cosmochimica Acta, 1954, Vol. 5, pp. 245 to 285. Pergamon Press Ltd., London

The geochemistry of some igneous rock series: Part II

S. R. Nockolds and R. Allen
Dept. of Mineralogy and Petrology, Cambridge, England

(*Received* 9 *February* 1954)

ABSTRACT

This paper concerns the distribution of some of the commoner trace elements with respect to the major elements in certain alkali igneous rock series. These include the rocks of the Scottish Tertiary alkali series, the Hawaiian alkali rocks, some of the Polynesian alkali series, and the latite series of the East Central Sierra Nevada.

Introduction

In this, the second of our series of papers concerning the behaviour of the commoner trace elements with respect to the major constituents in some well known igneous rock series, we propose to investigate their behaviour in certain alkali igneous rock series.

The method of investigation has been the same as that detailed in the first paper of this series (Nockolds and Allen, 1953), and the diagrams presented here are all of the same form, and on the same scale, as those given in that paper.

2. Alkali Igneous Rock Series

The following igneous rock series of alkali type have been examined: the Scottish Tertiary alkali series; the alkali rocks of the Hawaiian Islands; three of the four or five series of alkali igneous rocks found in the Polynesian Islands; and the latite series of the East Central Sierra Nevada. For comparison, we have the results of trace element determinations on the Braefoot Outer Sill as presented by Higazy (Higazy, 1952).

(a) *The Scottish Tertiary alkali series*

This is the well-known alkali basalt → mugearite → trachyte series of lavas and corresponding minor intrusions the members of which have been described in detail by officers of the Geological Survey of Great Britain and others (Harker, 1904 and 1908; Bailey *et al.*, 1924; Tyrrell, 1928). The chemical data available are, however, not as abundant as could be desired and are here supplemented by four new chemical analyses. A variation diagram showing the relationship between Mg, ($Fe'' + Fe'''$), and (Na + K), and between Ca, Na and K is given in Fig. 16. As in diagrams of this kind in the previous paper, the bulk of the rocks fall on a smooth curve and the rocks whose composition is believed to have been influenced to a greater or less degree by the process of crystal accumulation are separately distinguished. The approximate composition of the supposed parental magma will be found in Table 17, col. 1.

(b) *The Hawaiian alkali rocks*

The lavas of Hawaii have received much attention from petrographers and their chemistry is also well known, largely through the labours of Washington. The results of this research have recently been summarised and extended, for the island

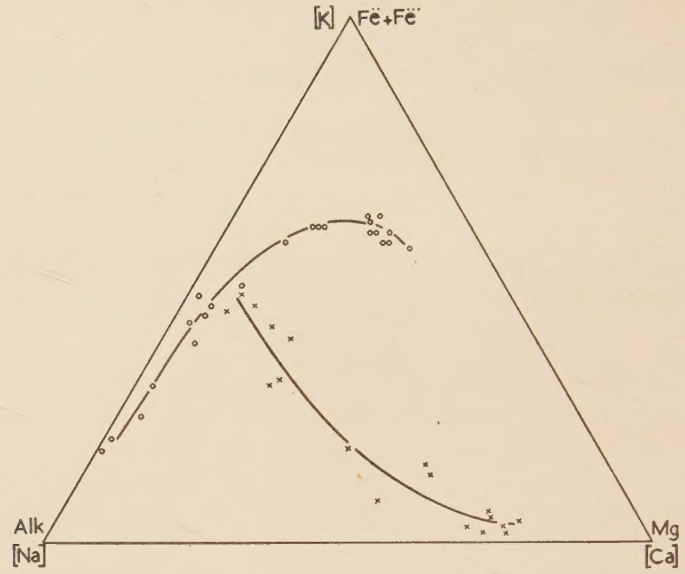

Fig. 16. Variation diagram of the rocks of the Scottish alkali basalt → trachyte series. Small circles refer to variation in (Fe″ + Fe‴), Mg, and (Na + K); crosses refer to variation in Ca, Na and K.

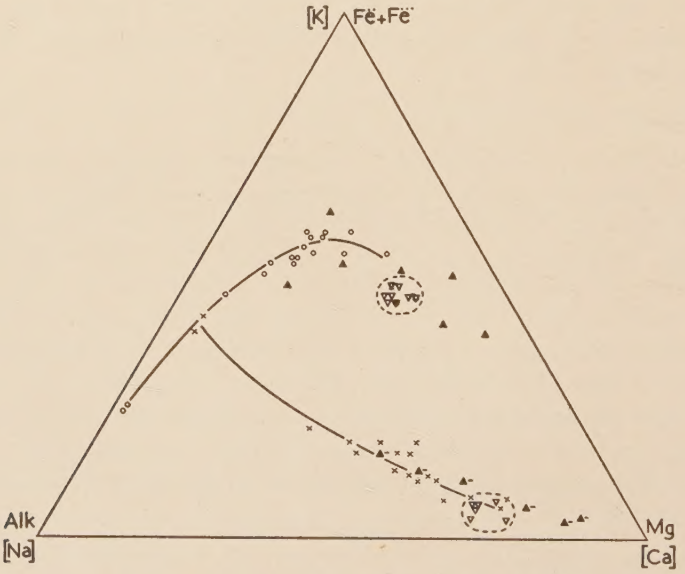

Fig. 17. Variation diagram of the rocks of the Hawaiian alkali basalt → trachyte series. Solid triangles refer to supposed accumulative rocks; open triangles enclosed by broken lines refer to rocks of the Honolulu series (Oahu).

of Hawaii, by MACDONALD (MACDONALD, 1949a). MACDONALD and POWERS have also detailed the characters of the rocks in the island of Maui (MACDONALD and POWERS, 1946), and MACDONALD has further considered the Hawaiian petrographic province as a whole (MACDONALD, 1949b). He does not, however, distinguish clearly between tholeiitic and alkali basalts both of which occur in the Hawaiian province, as pointed out by TILLEY (TILLEY, 1950). There is little doubt that the main series of Hawaiian alkali rocks, bearing as it does such a striking resemblance to that of the Scottish Tertiary and to the alkali basalt → trachyte series of Polynesia, has been derived, like them, from a parental alkali basalt. The tholeiitic basalts of the Hawaiian islands will thus not be considered here but will receive attention in our next paper concerning the tholeiitic igneous rock series.

The variation diagram for the Hawaiian assemblage alkali basalt → "andesine-andesite" → "oligoclase-andesite" → trachyte is shown in Fig. 17. The form of the curves is like that of Fig. 16 but the Mg-Fe-Alk curve lies below that of the Scottish series (cf. TILLEY, 1952, Fig. 2, p. 541) and the shape of the Ca-Na-K curves is somewhat different so that the end products of the Hawaiian series are less rich in K, relative to Na, than those of the Scottish series. The supposed composition of the parental magma is given in Table 17 col. 2.

Some late and very basic alkali rocks have been described recently from the island of Oahu as the Honolulu series (WINCHELL, 1947). These are mostly nepheline-melilite basalts, nepheline basalts and nepheline basanites, forming a very restricted group enclosed by the dotted lines in Fig. 17.

(c) *The Polynesian alkali basalt → trachyte series*

In his great monograph on the igneous rocks of Polynesia (LACROIX, 1927) and in a number of later papers, LACROIX has provided a wealth of petrographical and chemical data. He recognized three main rock series (LACROIX, 1927, p. 57): a series without nepheline, a series with nepheline and an intermediate series. His series without nepheline is divisible into two distinct series, one represented by the alkali basalt → trachyte series, the other by the rocks of Easter Island. The rocks of the Samoan islands provide the best example of his intermediate series, and it is possible that another intermediate series exists in addition. Unfortunately we have little material at our disposal from these intermediate series so we shall not discuss them further.

The rocks of the Polynesian alkali basalt → trachyte series are very similar to those of the Hawaiian Islands and the Scottish Tertiary, as may be seen from the variation diagram (Fig. 18). Here belong the igneous rocks of Gambier, Moorea, the Society Islands, the Marquesas (in part) and, with slight differences, those of Pitcairn. The Fe-Mg-Alk curve lies just above that for the Hawaiian series while the Ca-Na-K curve is practically parallel with that for the Hawaiian series but displaced somewhat upwards towards the K apex. It will be noted that the Ca-Na-K curve is here virtually a straight line while the curvature of the same curve in the Hawaiian series is feeble. This contrasts with the very definite curvature shown by the same curve in the Scottish Tertiary series. The approximate composition of the supposed parental magma is given in Table 17 col. 3.

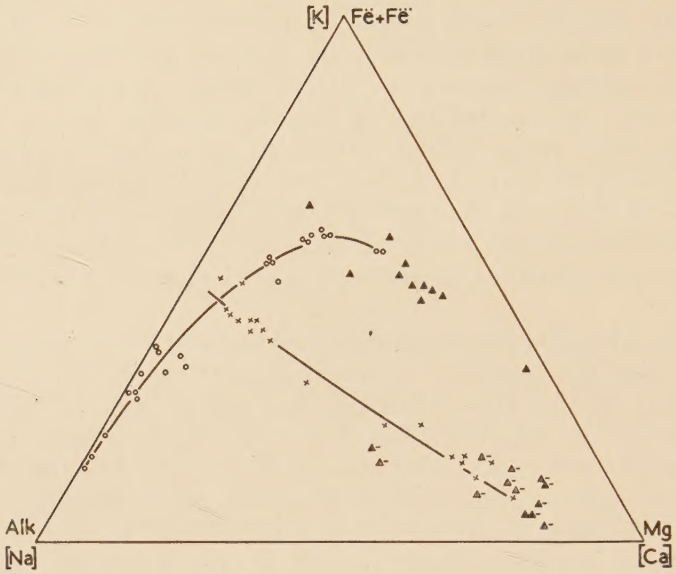

Fig. 18. Variation diagram of the rocks of the Polynesian alkali basalt → trachyte series.

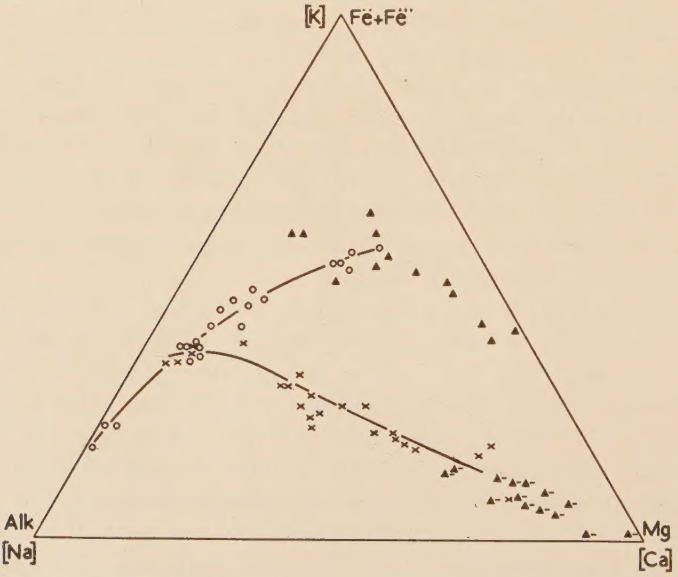

Fig. 19. Variation diagram of the rocks of the Polynesian alkali basalt → phonolite series.

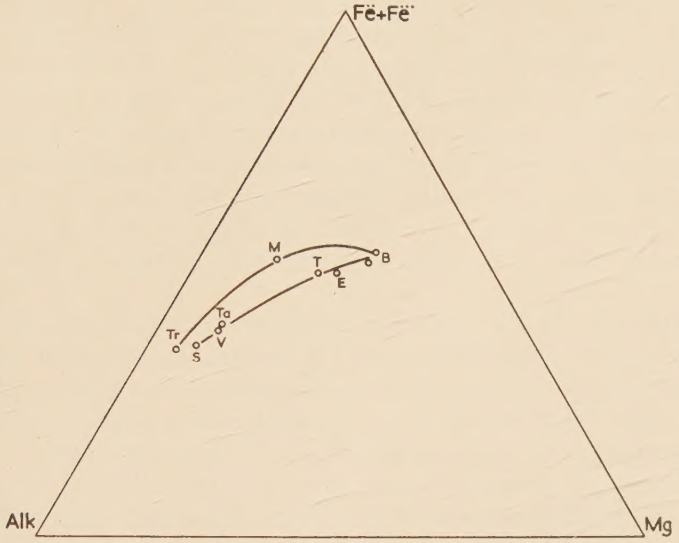

Fig. 20. Plot of certain average compositions of igneous rock types from the Scottish Carboniferous, taken from TOMKEIEFF (1937). B = basalt, M = mugearite, Tr = trachyte, E = essexite, T = teschenite, Ta = trachyandesite, V = vein in teschenite, S = syenite vein in essexite.

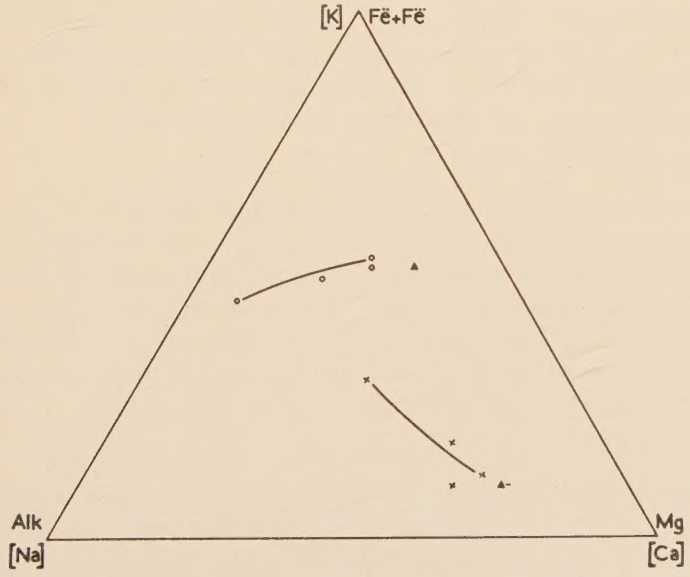

Fig. 21. Variation diagram of the rocks of the Circular Head laccolith.

(d) *The Polynesian alkali basalt → phonolite series*

The rocks of this series are best displayed in Tahiti and, to some extent, in the Marquesas. The form of the variation diagram (Fig. 19) is quite different from that shown by the alkali basalt → trachyte series. In particular, the Mg-Fe-Alk curve does not move towards the Fe-apex in its early stages but declines steadily away from the parental magma. In this respect the curve is like those shown by calc-alkali igneous rock series, while the behaviour of the alkali basalt → trachyte series is like that shown by many, though not all, tholeiitic rock series. The Ca-Na-K curve is also different. In the alkali basalt → trachyte series this curve is either a straight line or is concave towards the K-apex. Here the curve is concave towards the Na-apex.

That this difference in the variation diagrams of the two series is not confined to Polynesia may be readily discovered by plotting the average compositions of some of the various igneous types of the Scottish Carboniferous province (Tomkeieff, 1937). Fig. 20 shows the two series stemming from a common parental magma, as also appears to be the case with the Polynesian rocks.

A similar variation diagram is also given by the alkali rocks from the differentiated laccolith of Circular Head, Tasmania (Edwards, 1941) (Fig. 21).

(e) *The Polynesian (Easter Island) basalt → alkali rhyolite series*

The lavas of Easter Island have been described by Lacroix (Lacroix, 1936b) and Bandy (Bandy, 1937) and give the variation diagram shown in Fig. 22. The basalts of this series are relatively rich in iron as may be seen by comparing this Fig. with Figs. 18 and 19. Once again, this type of variation diagram appears to have close analogues elsewhere, for instance, in the lavas of the Piton des Neiges, Réunion (Lacroix, 1936a), whose variation diagram is intermediate, in some respects, between that for Easter Island and those of the typical basalt → trachyte series (Fig. 23). The basalt whose composition is given in Table 17 col. 8 may represent the parental magma but it is possible that the latter is more basic and unrepresented by the basalts analyzed so far from the island.

(f) *The Braefoot Outer Sill*

The various rock types present in this teschenite sill have been described by Campbell, Day and Stenhouse (Campbell, Day and Stenhouse, 1933) while the trace elements of the rocks have been determined recently by Higazy (Higazy, 1952) (see later). The variation diagram (Fig. 24) shows that the Fe-Mg-Alk curve is almost linear, and in this respect recalls the curve of the Polynesian basalt → phonolite series or that of the Circular Head laccolith. But, in contrast with these, the Ca-Na-K curve here is quite strongly concave upwards.

(g) *The East Central Sierra Nevada latite series*

Our final series of alkali igneous rocks is quite distinct from all the others, not only mineralogically and chemically, but also from the point of view of its environment and associates. We are again indebted to Dr. J. H. Halsey and Dr. D. B. Slemmons for allowing us to make use of their unpublished chemical analyses. This latite series, whose variation diagram is given in Fig. 25, is closely associated

Fig. 22. Variation diagram of the rocks of the Easter Island basalt → alkali rhyolite series.

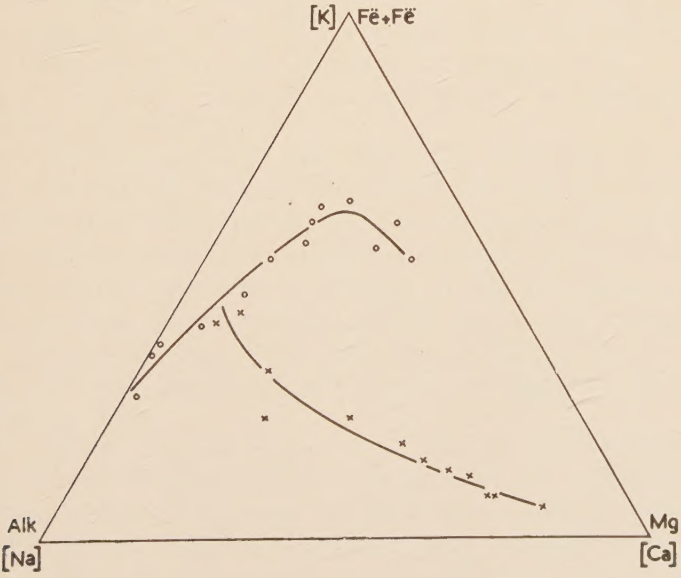

Fig. 23. Variation diagram of the rocks of Piton de Neiges, Réunion.

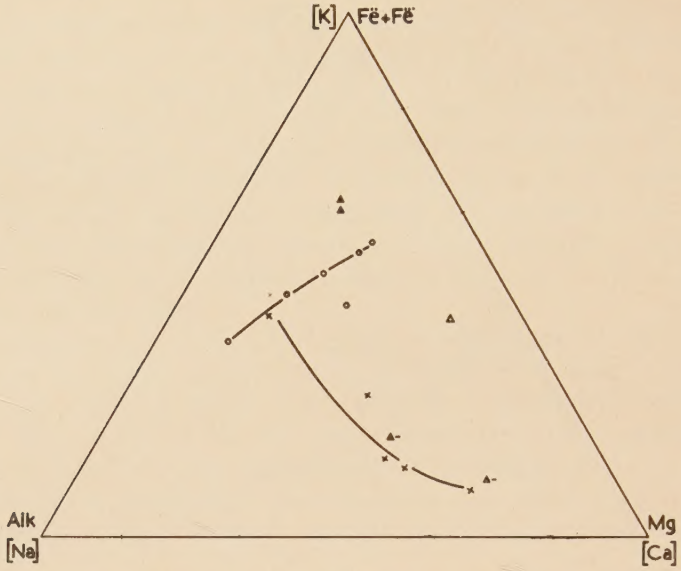

Fig. 24. Variation diagram of the rocks of the Braefoot Outer sill. Solid triangles refer to dolerite-pegmatites. Open triangle represents picroteschenite.

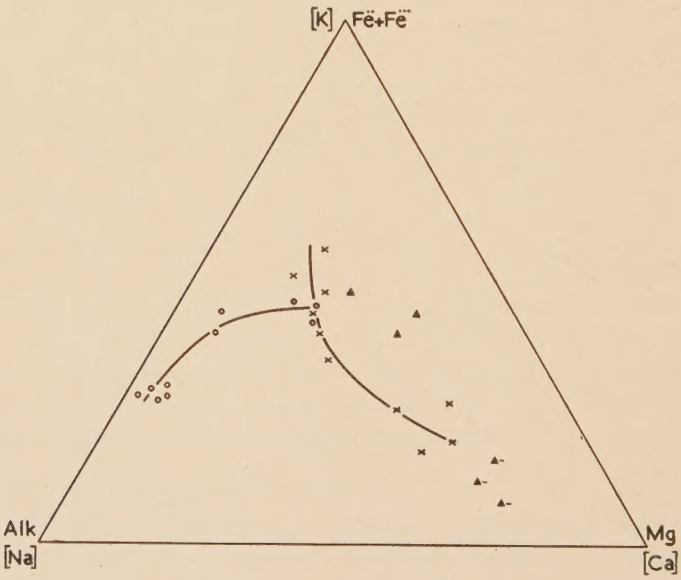

Fig. 25. Variation diagram of the rocks of the East Central Sierra Nevada latite series.

with the East Central Sierra Nevada calc-alkali series already investigated (Nockolds and Allen, 1953, p. 109). Halsey (personal communication) believes the parental magma of this series to have the composition given in Table 16 col. 1. Certain late basalts may be accumulative members of this series and three of these are shown in Table 16 cols. 7, 8 and 9.

Variation in the major and trace elements of the alkali rock series

The data on which the following discussion is based are given in Tables 10 to 16, so far as the trace elements are concerned. For the major elements we had, as in our previous paper, all the chemical data (recalculated on a water-free basis) available for each of the particular series. The diagrams illustrating the behaviour of the major, and some of the minor, elements along the supposed liquid line of descent in the various series are given in Figs. 26 to 29. They were prepared in the same way as those of our previous paper.

(a) *Alkali basalt → trachyte series of the Scottish Tertiary, Hawaii and Polynesia* (*Tables* 10, 11 *and* 12)

These three series are similar and may be considered together. A few determinations of the trace element concentrations in Hawaiian "andesine-andesite," "oligoclase-andesite" and trachyte have been made recently by Wager and Mitchell (Wager and Mitchell, 1953), who also investigated two mugearites and a trachyte from the Island of Skye. Their results agree well with those given here, except for Sr, Zr and Y in the higher concentration ranges, where their values are greater than ours. Their results for Hawaiian basalts will be mentioned in the next paper of this series as they are all tholeiitic types and do not belong to the rock series under consideration.

Silicon and Oxygen (*Figs.* 26*a*–26*c*). The behaviour of Si and O is practically identical in all three examples, the ratio of Si : O ranging from 1 : 2 at the basic end to 1 : 1·6, 1 : 1·56 and 1 : 1·5 at the acid end of the Hawaiian, Polynesian and Scottish series respectively.

Aluminium and Gallium (*Figs.* 26*a*–26*c*). The curves for Al show a slight, but steady, increase towards the acid end in the Hawaiian and Polynesian series, whereas the curve for Al passes through a feeble maximum in the Scottish series. The curves for Ga are practically parallel with those of Al, though there is a slight divergence at the acid end in the case of the Hawaiian and Polynesian series leading to a slight decrease in the Ga/Al ratio. The average ratio Ga × 1000/Al along the supposed liquid line of descent is 0·19 for the Polynesian series (0·27 for the few Pitcairn Island lavas), 0·24 for the Hawaiian series and 0·25 for the Scottish Tertiary series.

Magnesium, Nickel, Lithium, Iron, Cobalt, Chromium, Vanadium, Titanium (*Figs.* 27*a*–27*c*). These elements behave in the same way in each of the three series. Magnesium shows a steady decrease as the function $[(\frac{1}{3}\mathrm{Si} + \mathrm{K}) - (\mathrm{Ca} + \mathrm{Mg})]$ grows larger and lithium shows a relatively small increase, thus leading to an increase in the Li/Mg ratio. Chromium and nickel, on the other hand, show a rapid decrease and it is not long before they fall below the limit of sensitivity. Cobalt remains practically steady for a time and then decreases. As a result, the

Table 10. *Scottish Tertiary; basalt → trachyte series**

	1	2	3	4	5	6	7	8	9	10	11	12	13
Si	$218\cdot10^3$	$221\cdot10^3$	$218\cdot10^3$	$225\cdot10^3$	$243\cdot10^3$	$244\cdot10^3$	$236\cdot10^3$	$260\cdot10^3$	$279\cdot10^3$	$284\cdot10^3$	$309\cdot10^3$	$301\cdot10^3$	$322\cdot10^3$
Al	$86\cdot10^3$	$84\cdot10^3$	$85\cdot10^3$	$92\cdot10^3$	$79\cdot10^3$	$71\cdot10^3$	$86\cdot10^3$	$89\cdot10^3$	$88\cdot10^3$	$88\cdot10^3$	$86\cdot10^3$	$84\cdot10^3$	$85\cdot10^3$
Ti	$13\cdot10^3$	$13\cdot10^3$	$22\cdot10^3$	$17\cdot10^3$	$11\cdot10^3$	$12\cdot10^3$	$11\cdot10^3$	$11\cdot10^3$	$5\cdot10^3$	$5\cdot10^3$	$4\cdot10^3$	$3\cdot10^3$	$1\cdot10^3$
Fe‴	$24\cdot10^3$	$26\cdot10^3$	$26\cdot10^3$	$23\cdot10^3$	$38\cdot10^3$	$51\cdot10^3$	$43\cdot10^3$	$22\cdot10^3$	$22\cdot10^3$	$20\cdot10^3$	$22\cdot10^3$	$13\cdot10^3$	$7\cdot10^3$
Mg	$57\cdot10^3$	$41\cdot10^3$	$43\cdot10^3$	$26\cdot10^3$	$26\cdot10^3$	$24\cdot10^3$	$19\cdot10^3$	$7\cdot10^3$	$7\cdot10^3$	$7\cdot10^3$	$5\cdot10^3$	$4\cdot10^3$	$2\cdot10^2$
Fe″	$77\cdot10^3$	$81\cdot10^3$	$84\cdot10^3$	$84\cdot10^3$	$61\cdot10^3$	$51\cdot10^3$	$58\cdot10^3$	$47\cdot10^3$	$39\cdot10^3$	$20\cdot10^3$	$5\cdot10^3$	$28\cdot10^3$	$11\cdot10^3$
Na	$20\cdot10^3$	$23\cdot10^3$	$20\cdot10^3$	$38\cdot10^3$	$28\cdot10^3$	$29\cdot10^3$	$39\cdot10^3$	$47\cdot10^3$	$46\cdot10^3$	$61\cdot10^3$	$40\cdot10^3$	$44\cdot10^3$	$43\cdot10^3$
Ca	$64\cdot10^3$	$66\cdot10^3$	$60\cdot10^3$	$47\cdot10^3$	$53\cdot10^3$	$54\cdot10^3$	$39\cdot10^3$	$24\cdot10^3$	$21\cdot10^3$	$11\cdot10^3$	$11\cdot10^3$	$9\cdot10^3$	$7\cdot10^3$
K	$2\cdot10^3$	$6\cdot10^3$	$4\cdot10^3$	$6\cdot10^3$	$12\cdot10^3$	$15\cdot10^3$	$18\cdot10^3$	$32\cdot10^3$	$29\cdot10^3$	$33\cdot10^3$	$41\cdot10^3$	$46\cdot10^3$	$39\cdot10^3$
P	(900)	(1300)	(1300)	(2200)	(2200)	(2200)	(6500)	(2200)	(3100)	(2600)	(1400)	(1300)	(1300)
Ga	20	20	25	20	25	25	20	20	20	20	15	25	20
Cr	150	100	15	*	*	3	*	*	*	*	*	*	*
V	150	250	200	100	125	125	*	*	*	*	10	*	*
Li	25	20	15	20	15	20	30	50	40	60	40	25	50
Ni	125	65	50	*	5	*	*	*	*	*	*	*	*
Co	30	30	40	20	25	30	*	*	*	*	*	*	*
Sc	20	30	15	*	*	*	*	*	*	*	*	*	*
Zr	100	100	100	250	250	150	500	1000	300	550	300	550	400
Mn	(1400)	(3900)	(1500)	(1500)	(3100)	(3900)	(2300)	(1500)	(1500)	(4000)	(900)	(2300)	(3000)
Y	20	35	25	40	35	15	40	40	40	50	40	60	70
La	*	*	*	*	*	*	50	100	50	60	100	100	100
Sr	325	500	450	1250	500	500	1000	700	850	500	550	500	5
Pb	*	*	*	*	*	*	*	*	20	10	20	20	20
Ba	50	300	100	300	1000	1000	1500	2000	2250	1700	2500	2250	1500
Rb	5	15	10	25	60	70	50	100	125	100	150	150	150
F	—	—	—	—	500	500	1000	300			—	—	—
Fe	64	72	72	80	79	81	84	91	90	85	84	91	99
Mg	36	28	28	20	21	19	16	9	10	15	16	9	1
Fe	56	61	62	60	60	60	57	45	43	28	24	30	18
Mg	32	23	24	15	16	14	11	5	5	5	4	3	tr.
Alk	12	16	14	25	24	26	32	50	52	67	72	67	82
Position	−4·6	−2·7	−2·6	+0·8	+1·4	+1·8	+3·9	+8·8	+9·4	+11·0	+12·8	+13·3	+13·9

[Mo, Sn and Cs below their limits of sensitivity in every specimen.]

*All values in this and following tables in ppm. An asterisk denotes below limit of sensitivity.

Table 10A. *Scottish Tertiary; basalt → trachyte series*

	1	2	3	4	5	6	7	8	9	10	11	12	13
Ga × 1000/Al	0·23	0·24	0·29	0·22	0·32	0·35	0·23	0·22	0·23	0·23	0·18	0·30	0·24
Cr × 1000/Mg	2·6	2·4	0·3	*	*	0·1	*	*	*	*	*	*	*
V × 1000/Mg	2·6	6·1	4·7	3·8	4·8	5·2	*	*	*	*	2·0	*	*
Li × 1000/Mg	0·4	0·5	0·3	0·8	0·6	0·8	1·6	7·1	5·7	8·6	8·0	6·3	250
Ni × 1000/Mg	2·2	1·6	1·2	*	0·2	*	*	*	*	*	*	*	*
Co × 1000/Mg	0·5	0·7	0·9	0·8	1·0	1·2	*	*	*	*	*	*	*
Fe/Mg	1·8	2·6	2·6	4·1	3·8	4·2	5·3	9·9	8·7	5·7	5·4	10·2	90
Cr × 1000/Fe	1·5	0·9	0·1	*	*	0·03	*	*	*	*	*	*	*
V × 1000/Fe	1·5	2·3	1·8	0·9	1·3	1·2	*	*	*	*	0·4	*	*
Co × 1000/Fe	0·3	0·3	0·4	0·2	0·3	0·3	*	*	*	*	*	*	*
Y × 1000/Ca	0·3	0·5	0·4	0·9	0·7	0·3	1·0	1·7	1·9	4·5	3·6	6·7	10·0
Sr × 100/Ca	0·5	0·8	0·7	2·7	0·9	0·9	2·6	2·9	4·0	4·5	5·0	5·6	0·1
Sr × 100/Ca + K	0·5	0·7	0·7	2·4	0·8	0·7	1·8	1·3	1·7	1·1	1·1	0·9	0·01
Ba × 100/K	2·5	5·0	2·5	5·0	8·3	6·7	8·3	6·3	7·8	5·2	6·1	4·9	3·8
Rb × 100/K	0·25	0·25	0·25	0·4	0·5	0·5	0·3	0·3	0·4	0·3	0·4	0·3	0·4

1. Basalt, Fishnish, Mull. Unpublished analysis by J. H. Scoon.
2. Basalt, E. Slope of Orval, Rum. Harker (1908), Anal., p. 57.
3. Basalt, 200 yds W. of Lochaline Pier, Morven. Bailey *et al.* (1924), Anal. II, p. 15.
4. Mugearite-basalt, River Rha, Skye. Unpublished analysis by J. H. Scoon.
5. Doleritic mugearite, pass S. of Fionn-Chrò, Rum. Harker (1908), Anal., p. 130.
6. Mugearite, Eilean a'Bhaird, Canna Harbour, Canna. Harker (1908), Anal., p. 130.
7. Mugearite, Druim na Crìche, Skye. Harker (1904), Anal., p. 263.
8. Mugearite, E. of Kinloch Inn. Loch Scridain, Mull. Bailey *et al.* (1924), Anal. I, p. 27.
9. Mugearite, Totador, Skye. Unpublished analysis by J. H. Scoon.
10. Trachyte, 5 miles S.E. of Tobermory, Mull. Bailey *et al.* (1924), Anal. III, p. 27.
11. Trachyte, Bracadale, Skye. Unpublished analysis by J. H. Scoon.
12. Trachyte, plug in vent, W. of Salen, Mull. Bailey *et al.* (1924), Anal. IV, p. 27.
13. Orthophyre, Holy Island Sill, Arran. Tyrrell (1928), Anal. 18, p. 237.

Fig. 26*a–g*. Variation in silicon, oxygen, aluminium and gallium. Values in weight per cent, with Ga × 1000.

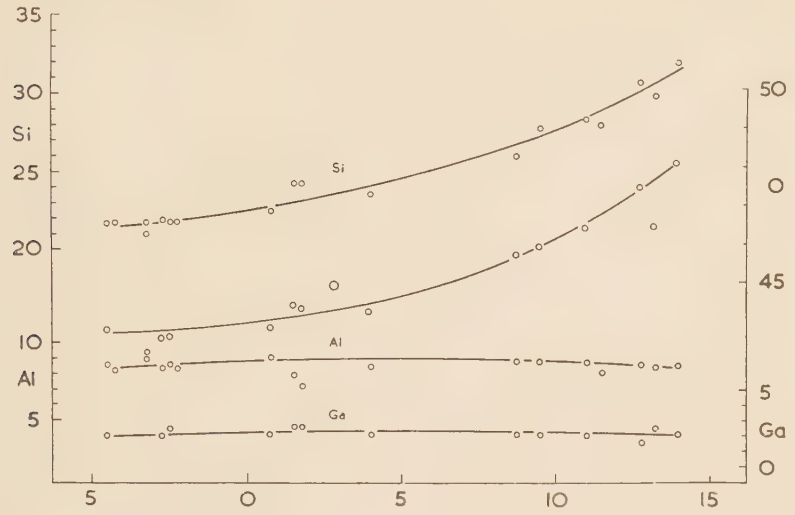

Fig. 26*a*. Scottish Tertiary alkali basalt → trachyte series.

Fig. 26*b*. Hawaiian alkali basalt → trachyte series.

Co curve cuts across the Ni curve in each case. The earliest rocks have Ni > Co but this is soon reversed and we have Ni < Co.

The curve for iron passes through a very feeble maximum towards the basic end of each series and then falls steadily. In this it is followed by titanium and by vanadium, where the maximum is more pronounced and where the fall in the curve is rapid once the maximum has been passed.

It should be noted that the curves for Cr and Ni fall to very low values at about the same time. V and Co are associated in the same way, but fall to low values at a later stage than Cr and Ni.

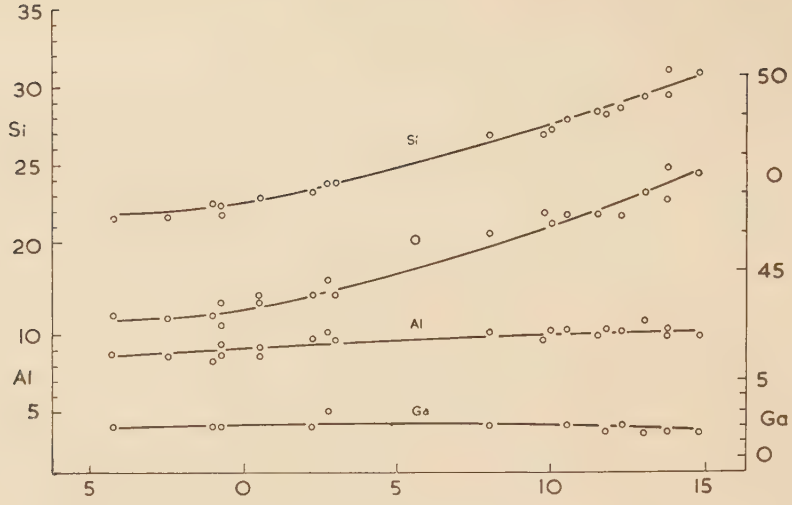

Fig. 26*c*. Polynesian alkali basalt → trachyte series.

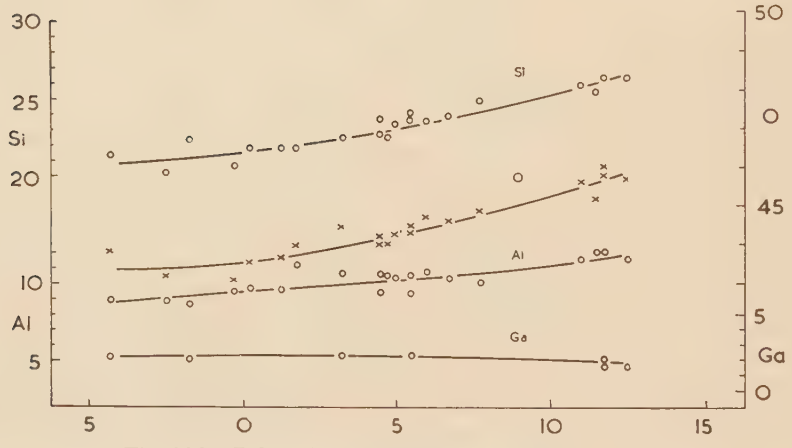

Fig. 26*d*. Polynesian alkali basalt → phonolite series.

There is a considerable contrast in the behaviour of some of these elements when compared with their behaviour in typical calc-alkali igneous rock series (Nockolds and Allen, 1953, p. 121). This point will be taken up more fully in our fourth paper.

The relationship between the trace elements and the major constituents is, again, very similar in all three rock series. The ratios Cr/Mg and V/Mg show a decrease as the function $[(\frac{1}{3}\mathrm{Si} + \mathrm{K}) - (\mathrm{Ca} + \mathrm{Mg})]$ increases, but this decrease is rather irregular. The ratio Cr/Fe, however, shows a steady decrease, while the ratio V/Fe decreases steadily likewise, after passing through a maximum towards the basic end, thus showing that Cr and V are associated with Fe rather than Mg.

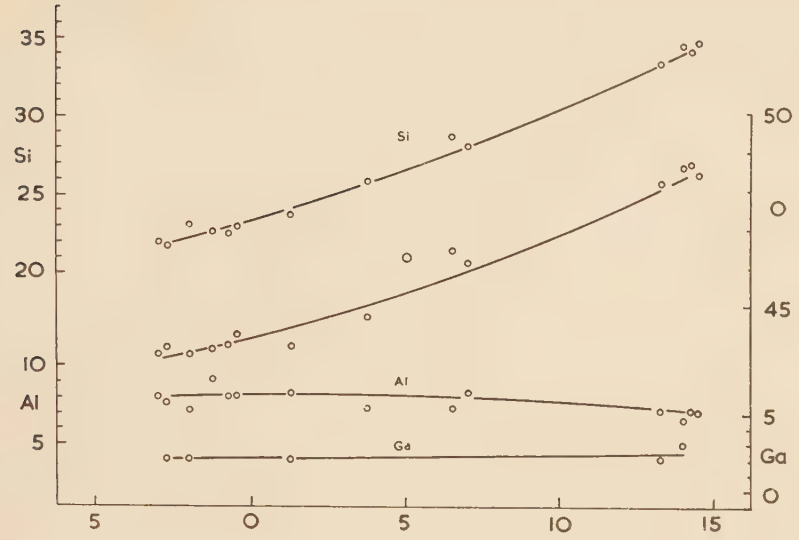

Fig. 26*e*. Easter Island basalt → alkali rhyolite series.

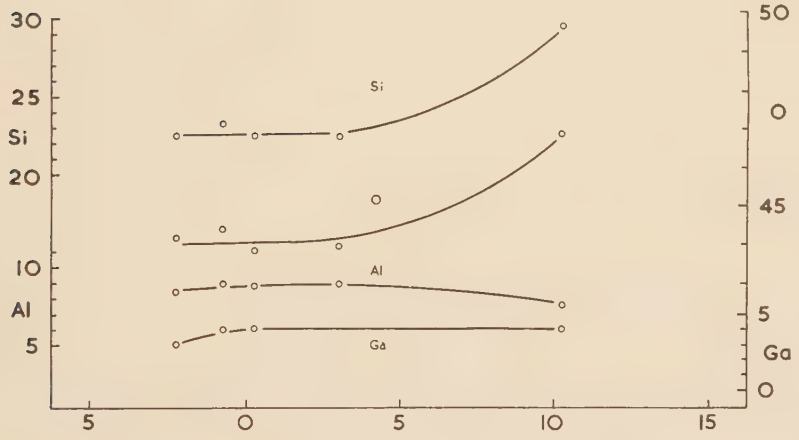

Fig. 26*f*. Braefoot Outer sill.

The ratio Ni/Mg decreases steadily in each series while, as already mentioned, the ratio Li/Mg increases on passing to the more acid rocks.

The ratios Co/Mg and Co/Fe show some slight differences in behaviour. In the Polynesian and Scottish Tertiary series both ratios are more or less constant, the ratio Co $\times$ 1000/Mg having values of 1·0 and 0·9, and the ratio Co $\times$ 1000/Fe having values of 0·3 and 0·3 respectively. These values compare closely with those already found for typical calc-alkali igneous rock series (Nockolds and Allen, 1953, p. 123). In the Hawaiian series, however, there appears to be a definite decrease in both the Co/Mg and Co/Fe ratios as the function [($\frac{1}{3}$Si + K) — (Ca + Mg)] increases.

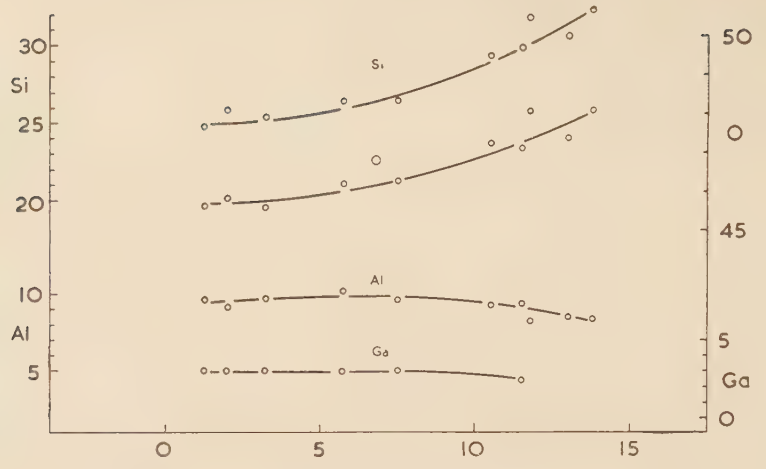

Fig. 26*g*. E. Central Sierra Nevada latite series.

Fig. 27*a–g*. Variation in chromium, lithium, magnesium, nickel, cobalt, iron and vanadium. Values in weight per cent with Cr, Li, Ni, Co and V × 1000 (except for Braefoot Outer Sill where scale for Cr, Ni and Co is reduced).

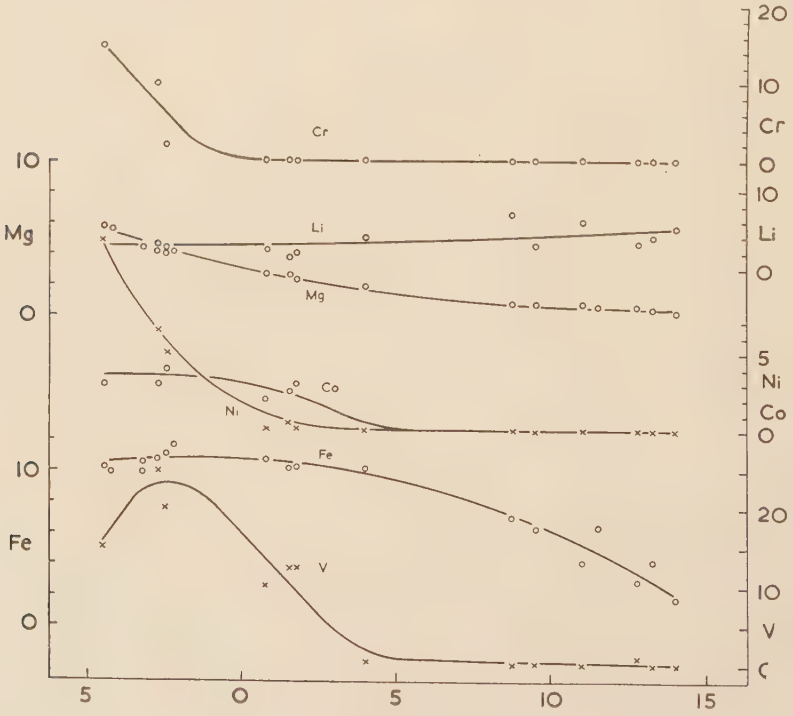

Fig. 27*a*. Scottish Tertiary alkali basalt → trachyte series.

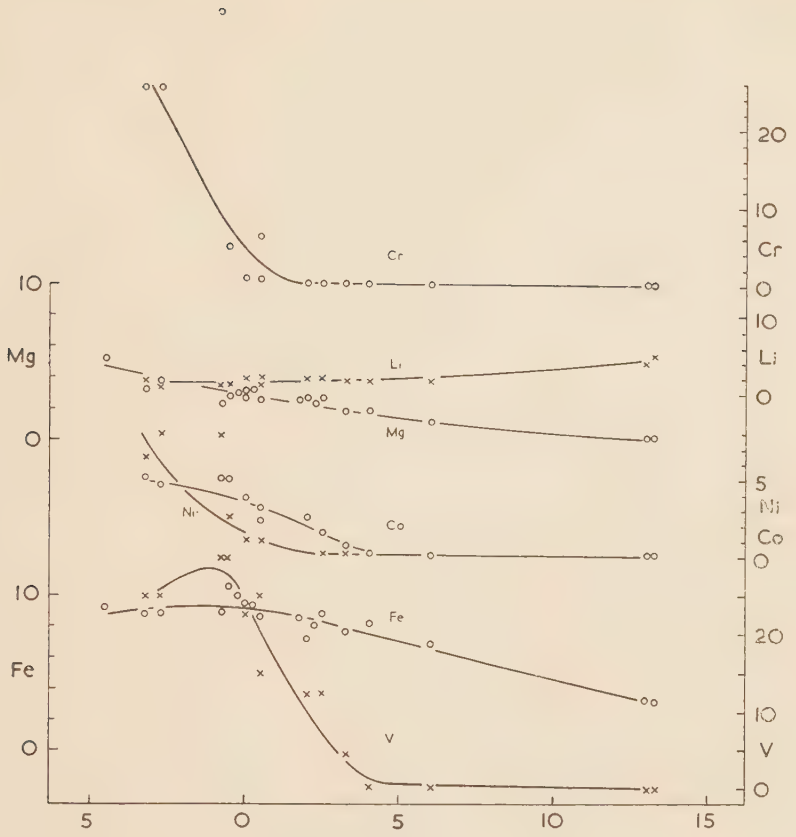

Fig. 27*b*. Hawaiian alkali basalt → trachyte series.

Calcium and Strontium (*Figs.* 28*a*–28*c*). Calcium decreases steadily in each series as the function $[(\frac{1}{3}\text{Si} + \text{K}) - (\text{Ca} + \text{Mg})]$ increases and, apart from the extreme basic end, the decrease is virtually linear as in calc-alkali igneous rock series. The absolute amounts of strontium present are closely similar in the Hawaiian and Polynesian series and definitely lower in the Scottish Tertiary series, but the form of the Sr curve is the same for all three series, gradually rising to a maximum and then declining to low values at the extreme acid end of each series.

The ratios Sr/Ca and Sr/Ca + K behave alike; in all three series they increase until late-stage rocks are reached, when they decline rapidly.

Yttrium. Yttrium does not show a great concentration in any of the rocks of the three series, but it does increase in amount in the later members. This increasing content, coupled with a decreasing content of Ca, leads to a marked increase in the Y/Ca ratio as the function $[(\frac{1}{3}\text{Si} + \text{K}) - (\text{Ca} + \text{Mg})]$ increases.

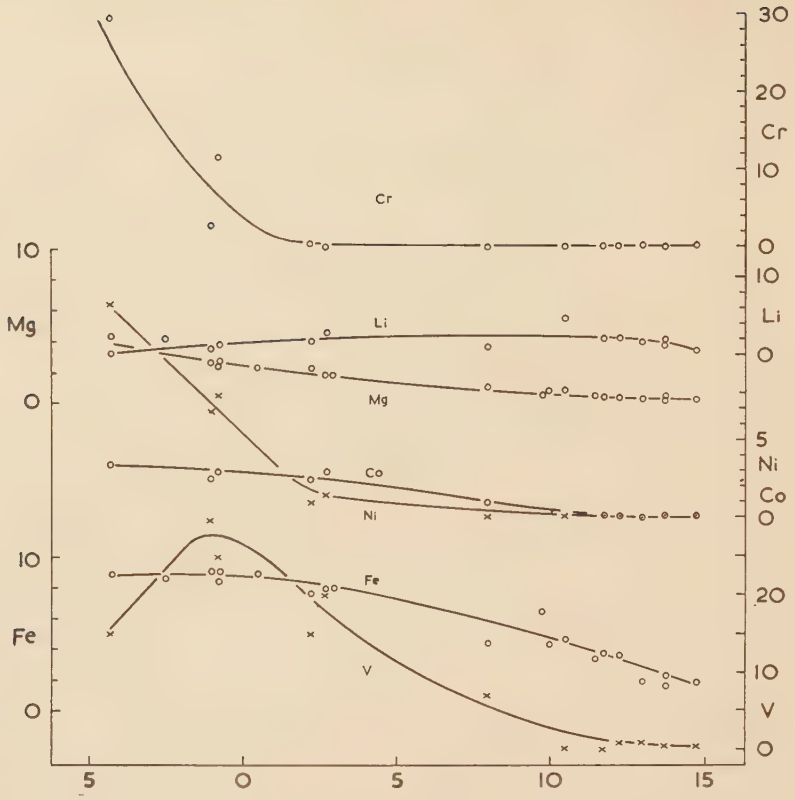

Fig. 27*c*. Polynesian alkali basalt → trachyte series.

Lanthanum. Lanthanum lies below the limit of sensitivity (40 ppm) at the basic end of each series. It appears in the intermediate and late-stage members but shows little evidence of concentration in the latter.

Sodium (*Figs.* 28*a*–28*c*). Sodium increases gradually in all three series as the function $[(\frac{1}{3}\mathrm{Si} + \mathrm{K}) - \mathrm{Ca} + \mathrm{Mg})]$ grows larger, but shows a slight drop in the extreme late-stage rocks of the Scottish Tertiary series.

Potassium, Barium, Rubidium, Caesium, Lead (*Figs.* 28*a*–28*c*). The curve for potassium rises steadily in each of the three series on passing from early basic to late-stage members, and the content of K in the latter does not differ much, in spite of the fact that the parental magma of the Scottish Tertiary series carries less K than those of the Hawaiian and Polynesian series (see Table 17).

Barium, like strontium, increases steadily in all three series and reaches a maximum, after which it declines. But the maximum is more pronounced than in the case of Sr, it is reached at a later stage, and the decline from the maximum is more rapid.

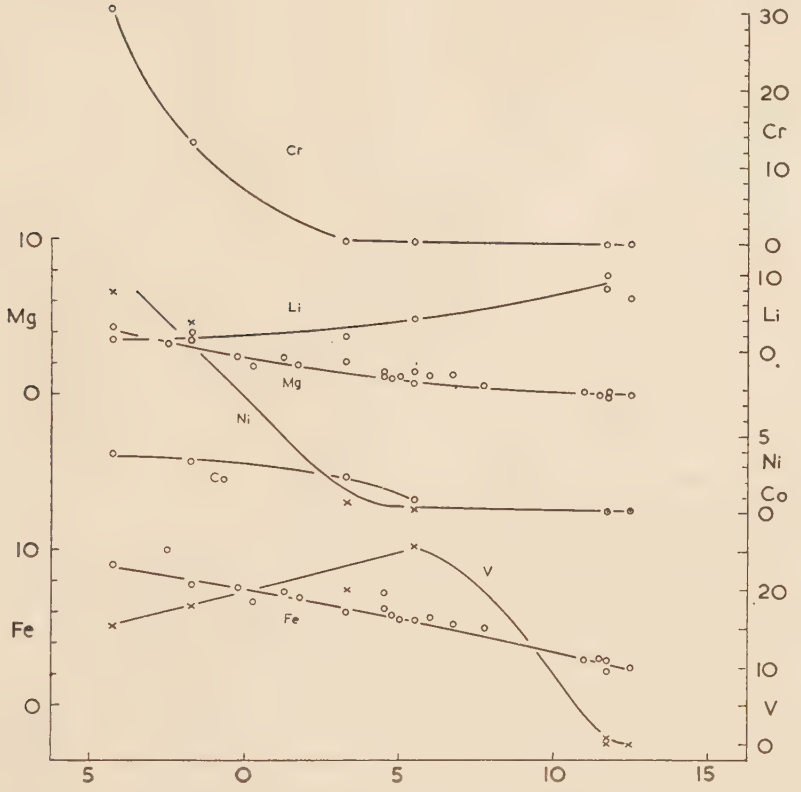

Fig. 27*d*. Polynesian alkali basalt → phonolite series.

The Ba/K ratio changes little in the Hawaiian and Polynesian series until the late-stage members are reached, when it decreases. In the Scottish Tertiary series this ratio appears to pass through a maximum and it is still relatively high when the late-stage types are reached. It must be noted, however, that this series is richer in Ba than the other two, and the late-stage members here are close to the maximum on the Ba curve. More extreme differentiates, if such exist, might well show a rapid decline in the Ba/K ratio.

The rubidium curve follows that for potassium in the Hawaiian and Polynesian series but, again, the Scottish Tertiary series behaves differently and the curve for Rb increases less sharply than that for K. Moreover the ratio Rb/K is different. In the first two series the ratio Rb × 100/K averages 0·5 and 0·8 respectively, whereas in the Scottish Tertiary it averages 0·35.

Caesium has not been found to rise above the limit of sensitivity (10–15 ppm) in any of the rocks in these series.

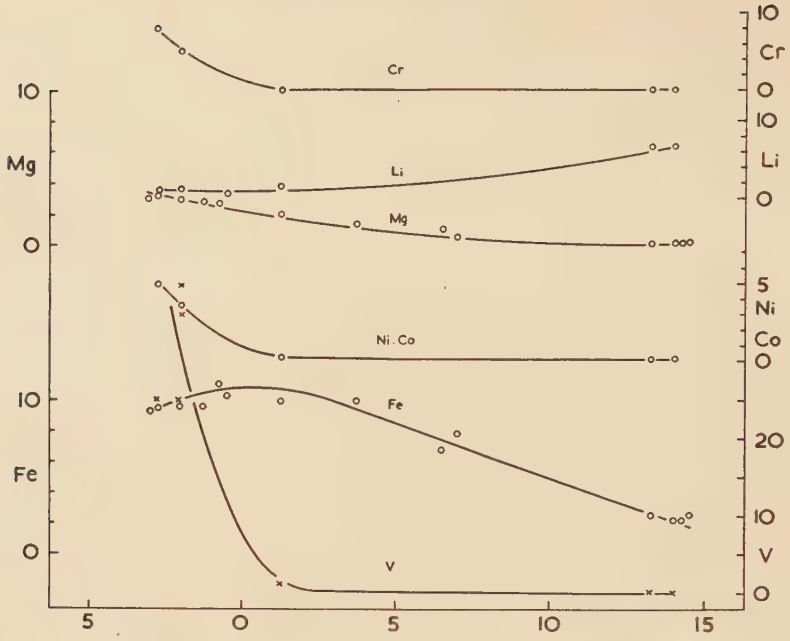

Fig. 27*e*. Easter Island basalt → alkali rhyolite series.

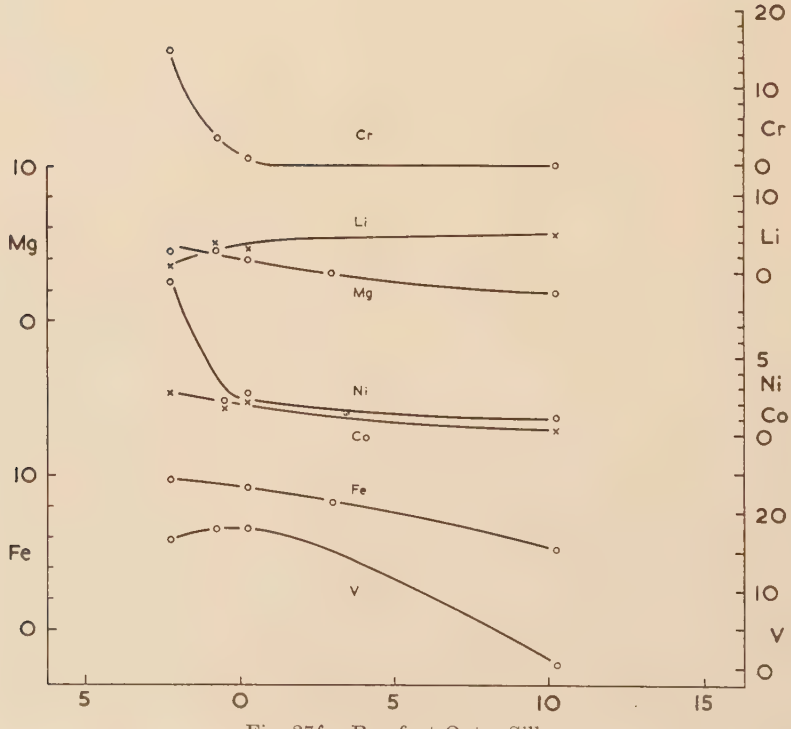

Fig. 27*f*. Braefoot Outer Sill.

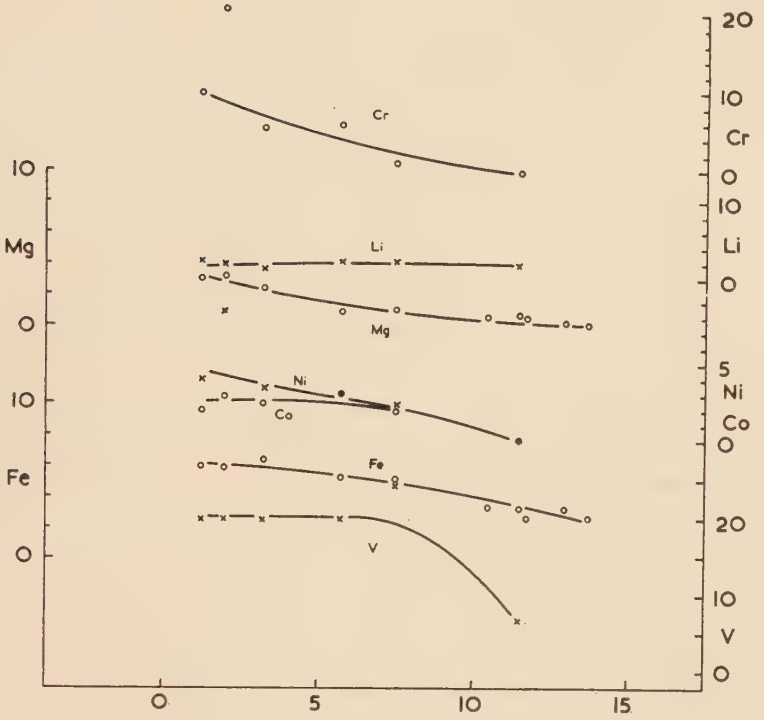

Fig. 27*g*. E. Central Sierra Nevada latite series.

Lead, as would be expected, is below the limit of sensitivity in all the basic rocks of each series. It appears in small amounts in the intermediate and late-stage members but never becomes at all highly concentrated.

Zirconium (*Fig.* 29). Zirconium increases in each series as we proceed from the early basic to the late-stage members and, unlike its behaviour in calc-alkali igneous rock series (see Nockolds and Allen, 1953, Fig. 14, p. 140), does not pass through a gentle maximum in the intermediate stages.

Molybdenum. Molybdenum shows its presence quite regularly, though only in small amount, in the late-stage members of the Hawaiian and Polynesian series. It was not detected in any rocks of the Scottish Tertiary series.

The lavas of Pitcairn Island, marked with an asterisk in Table 12, differ in some respects from the other lavas dealt with here, though clearly belonging to the same general types. Among the major constituents the main difference is to be seen in their greater richness in iron, and their trace element contents are also significantly different. Unfortunately we have not had enough samples to follow out these differences in detail.

Table 11. *Hawaiian Islands; basalt → trachyte series*

	1	2	3	4	5	6	7	8	9	10	11	12	13	14	15	16
Si	200·10³	222·10³	225·10³	231·10³	229·10³	221·10³	224·10³	220·10³	224·10³	233·10³	237·10³	242·10³	246·10³	254·10³	292·10³	293·10³
Al	57·10³	89·10³	82·10³	78·10³	75·10³	88·10³	86·10³	88·10³	94·10³	103·10³	87·10³	86·10³	91·10³	95·10³	93·10³	100·10³
Ti	15·10³	19·10³	21·10³	25·10³	19·10³	24·10³	25·10³	23·10³	20·10³	15·10³	16·10³	18·10³	13·10³	11·10³	2·10³	2·10³
Fe‴	30·10³	18·10³	18·10³	31·10³	30·10³	38·10³	31·10³	31·10³	40·10³	5·10³	41·10³	19·10³	25·10³	27·10³	12·10³	30·10³
Mg	91·10³	32·10³	37·10³	23·10³	28·10³	26·10³	31·10³	26·10³	25·10³	26·10³	26·10³	19·10³	19·10³	11·10³	2·10³	2·10³
Fe″	76·10³	68·10³	69·10³	57·10³	75·10³	57·10³	65·10³	55·10³	44·10³	66·10³	48·10³	58·10³	57·10³	42·10³	21·10³	1·10³
Na	12·10³	23·10³	27·10³	33·10³	25·10³	32·10³	31·10³	33·10³	35·10³	36·10³	35·10³	42·10³	40·10³	47·10³	61·10³	52·10³
Ca	88·10³	81·10³	74·10³	70·10³	64·10³	60·10³	54·10³	61·10³	57·10³	49·10³	46·10³	47·10³	41·10³	35·10³	6·10³	6·10³
K	3·10³	7·10³	9·10³	8·10³	11·10³	13·10³	11·10³	20·10³	13·10³	16·10³	18·10³	17·10³	18·10³	22·10³	42·10³	42·10³
B	—	*	—	*	—	—	—	—	—	2	—	15	—	—	10	—
P	(1440)	(2300)	(1000)	(1900)	(4000)	(3100)	(2660)	(3450)	(3800)	(3400)	(750)	(5500)	(2700)	(2660)	(600)	(1050)
Ga	15	20	20	25	20	25	25	25	25	20	20	20	20	20	15	15
Cr	1100	250	250	350	50	*	*	65	*	*	*	*	*	*	5	*
V	400	250	250	300	300	225	225	250	150	125	125	45	*	*	*	*
Mo	*	*	*	*	*	*	*	*	*	*	*	*	*	*	7	5
Li	5	15	10	10	10	15	10	15	5	15	15	15	15	20	45	50
Ni	300	65	80	80	25	10	10	25	10	*	*	*	*	*	8	*
Co	70	50	50	50	50	35	35	30	20	25	15	5	*	*	*	*
Sc	30	*	*	—	*	*	*	*	*	*	*	*	*	*	*	*
Zr	120	300	200	250	350	250	270	270	250	550	500	500	700	350	1000	700
Mn	(460)	(1250)	(950)	(750)	(1300)	(540)	(620)	(540)	(620)	(1150)	(1700)	(850)	(1250)	(620)	(2400)	(1150)
Y	20	30	25	35	35	40	45	35	35	50	40	50	40	45	50	50
La	*	*	*	*	*	*	*	*	*	?50	*	60	100	75	100	100
Sr	600	1000	1000	1000	1250	1250	1000	1500	1200	1750	1250	2000	1500	2000	30	40
Pb	*	*	*	*	*	*	*	*	*	*	10	10	10	*	30	?5
Ba	450	450	350	375	600	800	650	800	750	750	650	800	1000	1500	600	600
Rb	10	50	?5	25	80	100	70	100	70	80	80	75	30	100	350	300
Fe	54	73	70	79	79	79	76	77	77	73	77	80	81	86	93	94
Mg	46	27	30	21	21	21	24	23	23	27	23	20	19	14	7	6
Fe	50	58	54	58	62	57	57	52	53	48	53	50	52	46	24	25
Mg	43	22	23	15	17	16	18	16	16	17	15	12	12	8	2	2
Alk	7	20	23	27	21	27	25	32	31	35	32	38	36	46	74	73
Position	−10·9	−3·2	−2·7	−0·8	−0·5	+0·1	+0·1	+0·6	+0·6	+1·9	+2·5	+3·2	+4·0	+6·1	+13·1	+13·2

[Sn and Cs below their limits of sensitivity in every specimen.]

Table 11A. Hawaiian Islands; basalt → trachyte series

	1	2	3	4	5	6	7	8	9	10	11	12	13	14	15	16
Ga × 1000/Al	0·26	0·22	0·24	0·32	0·27	0·28	0·29	0·28	0·27	0·19	0·23	0·23	0·22	0·21	0·16	0·15
Cr × 1000/Mg	12	7·8	6·8	15	1·8	*	*	2·5	*	*	*	*	*	*	2·5	*
V × 1000/Mg	4·4	7·8	6·8	13	10·7	8·7	7·3	9·6	6·0	4·8	4·8	2·4	*	*	*	*
Li × 1000/Mg	0·05	0·5	0·3	0·4	0·4	0·6	0·3	0·6	0·2	0·6	0·6	0·8	0·8	1·8	22	25
Ni × 1000/Mg	3·3	2·0	2·2	3·5	0·9	0·4	0·3	1·0	0·4	*	*	*	*	*	4·0	*
Co × 1000/Mg	0·8	1·6	1·4	2·2	1·8	1·3	1·1	1·2	0·8	1·0	0·6	0·3	*	*	*	*
Fe/Mg	1·2	2·7	2·4	3·8	3·8	3·7	3·1	3·3	3·4	2·7	3·4	4·1	4·3	6·3	16	15
Cr × 1000/Fe	10·4	2·9	2·9	4·0	0·5	*	*	0·75	*	*	*	*	*	*	0·2	*
V × 1000/Fe	3·8	2·9	2·9	3·4	2·9	2·4	2·3	2·9	1·8	1·8	1·4	0·6	*	*	*	*
Co × 1000/Fe	0·7	0·6	0·6	0·6	0·5	0·4	0·4	0·3	0·2	0·4	0·2	0·1	*	*	*	*
Y × 1000/Ca	0·2	0·4	0·3	0·5	0·5	0·7	0·8	0·6	0·6	1·0	0·9	1·1	1·0	1·3	8·3	8·3
Sr × 100/Ca	0·7	1·2	1·4	1·4	2·0	2·1	1·9	2·5	2·1	3·6	2·7	4·3	3·7	5·7	0·5	0·7
Sr × 100/Ca + K	0·7	1·1	1·2	1·3	1·7	1·7	1·5	1·9	1·7	2·7	2·0	3·1	2·5	3·5	0·06	0·08
Ba × 100/K	15	6·4	3·9	4·7	5·5	6·2	5·9	4·0	5·8	4·7	3·6	4·7	5·6	6·8	1·4	1·4
Rb × 100/K	0·3	0·7	*	0·3	0·7	0·8	0·6	0·5	0·5	0·5	0·4	0·4	0·2	0·5	0·8	0·7

1. Picrite-basalt, 0·3 miles N. of Pakaoa Hill, Maui (Haleakala volcano). [Accumulative.] MACDONALD and POWERS (1946) Anal. 1, p. 119.

2. Olivine basalt, Papalele Gulch, N.E. side of Mauna Kea, Hawaii. MACDONALD (1949), Anal. 4, p. 38.

3. Olivine basalt, gulch near Kawaihoe, Kohala, Hawaii (Kohala volcano). MACDONALD (1949), Anal. 5, p. 87.

4. Porphyritic olivine basalt, Momouala Gulch, S. Slope of Kohala Mt., Hawaii (Kohala volcano). MACDONALD (1949), Anal. 8, p. 87.

5. Andesine andesite, Papalele Gulch, N.E. side of Mauna Kea, Hawaii. MACDONALD (1949), Anal. 7, p. 83.

6. Andesite, quarry on bank of Kalialinui Gulch, Maui (Haleakala volcano). MACDONALD and POWERS (1946), Anal. 3, p. 119.

7. Andesite, quarry 3·6 miles S.E. of Kahului, Maui (Haleakala volcano). MACDONALD and POWERS (1946), Anal. 5, p. 119.

8. Andesite, N. of Summit Rest House, Maui (Haleakala volcano). MACDONALD and POWERS (1946), Anal. 2, p. 119.

9. Andesite, 6 ft dyke in face of Kalahaku cliff, Maui (Haleakala volcano). MACDONALD and POWERS (1946), Anal. 4, p. 119.

10. Andesine andesite, highway N.W. of Nohonaohoe Cove, Mauna Kea, Hawaii. MACDONALD (1949), Anal. 9, p. 83.

11. Andesine andesite, Laupahoehoe Peninsula, N.E. side of Mauna Kea, Hawaii. MACDONALD (1949), Anal. 10, p. 83.

12. Oligoclase andesite, W. side of Moruoaloa Gulch, S. side of Kohala Mt., Hawaii (Kohala volcano). MACDONALD (1949), Anal. 11, p. 87.

13. Oligoclase andesite, highway cut at Puu Makea, S.W. slope of Kohala Mt., Hawaii (Kohala volcano). MACDONALD (1949), Anal. 12, p. 87.

14. Oligoclase andesite, 0·6 miles N.W. of Summit Rest House, W. rim of Haleakala crater, Maui (Haleakala volcano). MACDONALD and POWERS (1946), Anal. 6, p. 119.

15. Trachytic obsidian, Puu Waawaa, N.W. slope of Hualalai, Hawaii. MACDONALD (1949), Anal. 9, p. 78.

16. Trachyte, Highway 3 miles N. of Puu Waawaa, Hawaii. MACDONALD (1949), Anal. 8, p. 78.

Table 12. Polynesia; basalt → trachyte series

	1	2	3	4	5	6	7*	8	9*	10	11	12	13*	14	15	16*	17	18	19
Si	194·10³	218·10³	213·10³	215·10³	225·10³	223·10³	223·10³	231·10³	238·10³	268·10³	278·10³	280·10³	295·10³	284·10³	292·10³	305·10³	292·10³	308·10³	307·10³
Al	24·10³	63·10³	69·10³	89·10³	82·10³	94·10³	95·10³	97·10³	101·10³	101·10³	102·10³	103·10³	88·10³	101·10³	107·10³	83·10³	102·10³	97·10³	97·10³
Ti	4·10³	14·10³	20·10³	17·10³	26·10³	19·10³	23·10³	17·10³	15·10³	7·10³	4·10³	4·10³	5·10³	5·10³	4·10³	4·10³	4·10³	2·10³	2·10³
Fe‴	22·10³	26·10³	62·10³	32·10³	46·10³	57·10³	34·10³	31·10³	36·10³	32·10³	36·10³	25·10³	15·10³	31·10³	15·10³	6·10³	14·10³	13·10³	15·10³
Mg	200·10³	77·10³	65·10³	44·10³	26·10³	23·10³	22·10³	22·10³	17·10³	10·10³	8·10³	3·10³	2·10³	1·10³	7·10²	6·10²	11·10²	4·10²	3·10²
Fe″	82·10³	62·10³	40·10³	57·10³	44·10³	26·10³	71·10³	43·10³	42·10³	10·10³	10·10³	11·10³	33·10³	5·10³	4·10³	4·10³	10·10³	2·10³	3·10³
Na	6·10³	16·10³	15·10³	19·10³	24·10³	20·10³	26·10³	29·10³	36·10³	43·10³	42·10³	40·10³	44·10³	46·10³	50·10³	45·10³	45·10³	47·10³	45·10³
Ca	35·10³	81·10³	69·10³	78·10³	72·10³	75·10³	51·10³	57·10³	50·10³	31·10³	18·10³	20·10³	14·10³	16·10³	11·10³	12·10³	10·10³	9·10³	5·10³
K	3·10³	5·10³	9·10³	8·10³	13·10³	17·10³	12·10³	24·10³	15·10³	32·10³	36·10³	48·10³	39·10³	45·10³	46·10³	42·10³	52·10³	44·10³	50·10³
P	(220)	(700)	(1050)	(1130)	(2050)	(2340)	(1790)	(2925)	(830)	(2445)	(480)	(520)	—	(830)	(350)	—	(395)	(220)	(305)
Ga	5	10	15	20	20	20	25	20	30	20	20	15	20	20	15	25	15	15	15
Cr	1750	900	500	300	30	120	320	5	*	*	*	*	*	*	2	*	*	*	*
V	110	280	250	150	300	250	400	150	200	70	*	10	*	10	10	*	10	*	8
Mo	*	*	*	*	*	*	*	*	*	2	*	*	5	2	*	2	5	5	8
Li	1	10	10	10	10	15	10	20	30	10	50	20	50	20	15	50	25	10	5
Ni	2000	550	450	140	70	80	200	10	15	10	*	*	*	*	10	*	15	*	*
Co	220	80	55	35	25	30	70	25	30	10	*	*	*	*	*	*	*	*	*
Sc	—	—	—	—	—	—	—	—	—	—	—	—	—	—	—	—	—	—	—
Zr	40	100	175	175	200	225	300	320	550	550	500	300	500	500	500	650	600	500	500
Mn	—	(1470)	(1470)	(1390)	(770)	(1935)	(1160)	(2015)	(1160)	(1160)	(770)	(1320)	(775)	(1315)	(620)	(545)	(1550)	(310)	(1005)
Y	*	15	20	20	25	25	30	30	55	40	40	20	55	30	30	50	20	30	40
La	*	*	*	*	*	*	*	*	*	100	100	75	150	100	80	100	55	55	100
Sr	50	800	350	500	700	1000	800	2000	1500	2000	300	800	150	800	500	40	300	25	80
Pb	*	*	*	*	*	*	*	*	*	*	10	10	10	10	15	10	20	15	30
Ba	10	100	300	200	550	650	150	800	600	1000	1000	1200	2500	1600	1600	250	400	25	100
Rb	*	10	50	5	100	100	*	250	150	250	250	500	250	400	450	350	500	450	350
Fe	34	53	61	67	78	78	83	77	82	81	85	92	96	97	96	99	96	97	98
Mg	66	47	39	33	22	22	17	23	18	19	15	8	4	3	4	1	4	3	2
Fe	33	48	53	55	59	58	64	49	53	33	35	28	36	28	16·5	32·5	20	14	16
Mg	64	41	34	28	17	16	13	15	12	8	6	2	1·5	1	0·5	0·5	1	0·5	tr.
Alk	3	11	13	17	24	26	23	36	35	59	59	70	62·5	71	83	67	79	85·5	84
Position	−16·7	−8·0	−5·4	−4·2	−1·0	−0·7	+1·3	+2·2	+2·7	+8·0	+10·4	+11·8	+12·1	+12·3	+13·1	+13·1	+13·8	+13·8	+14·7

[Sn and Cs below their limits of sensitivity in every specimen.]

Table 12A. Polynesia; basalt → trachyte series

	1	2	3	4	5	6	7*	8	9*	10	11	12	13*	14	15	16*	17	18	19
Ga × 1000/Al	0·21	0·16	0·22	0·22	0·24	0·21	[0·26]	0·21	[0·30]	0·20	0·20	0·15	[0·23]	0·20	0·14	[0·30]	0·15	0·15	0·15
Cr × 1000/Mg	8·7	11·7	7·7	6·8	1·2	5·2	[14·5]	0·2	[*]	*	*	*	[*]	*	3	[*]	*	*	*
V × 1000/Mg	0·5	3·6	3·8	3·4	11·5	10·9	[18·2]	6·8	[11·8]	7·0	*	3·3	[*]	10	14	[*]	9	*	27
Li × 1000/Mg	0·01	0·1	0·2	0·2	0·4	0·7	[0·5]	0·9	[1·8]	1·0	6·2	6·7	[25]	20	21	[83]	23	25	17
Ni × 1000/Mg	10	7·1	6·9	3·2	2·7	3·5	[9·1]	0·5	[0·9]	1·0	*	*	[*]	*	14	[*]	14	*	*
Co × 1000/Mg	1·1	1·0	0·8	0·8	1·0	1·3	[3·2]	1·1	[1·8]	1·0	*	*	[*]	*	*	[*]	*	*	*
Fe/Mg	0·5	1·1	1·6	2·0	3·5	3·6	[4·8]	3·4	[4·6]	4·2	5·7	12	[24]	36	27	[17]	22	37	60
Cr × 1000/Fe	16·8	10·2	4·9	3·4	0·3	1·4	[3·0]	0·07	[*]	*	*	*	[*]	*	0·1	[*]	*	*	*
V × 1000/Fe	1·1	3·2	2·5	1·7	3·3	3·0	[3·8]	2·0	[2·6]	1·7	*	0·3	[*]	0·3	0·5	[*]	0·4	*	0·4
Co × 1000/Fe	2·1	0·9	0·5	0·4	0·3	0·4	[0·7]	0·3	[0·4]	0·2	*	*	[*]	*	*	[*]	*	*	*
Y × 1000/Ca	*	0·2	0·3	0·2	0·3	0·3	[0·6]	0·5	[1·1]	1·3	2·2	1·0	[3·9]	1·9	2·7	[4·2]	2·0	3·3	8·0
Sr × 100/Ca	0·1	1·0	0·5	0·6	1·0	1·3	[1·6]	3·5	[3·0]	6·5	1·7	4·0	[1·1]	5·0	4·5	[0·3]	3·0	0·3	1·6
Sr × 100/Ca + K	0·1	0·9	0·4	0·6	0·8	1·1	[1·3]	2·5	[2·3]	3·2	0·6	1·2	[0·3]	1·3	0·9	[0·1]	0·5	0·05	0·15
Ba × 100/K	0·3	2·0	3·3	2·5	4·2	3·8	[1·3]	3·3	[4·0]	3·1	2·8	2·5	[6·4]	3·6	3·5	[0·6]	0·8	0·06	0·2
Rb × 100/K	*	0·2	0·6	0·1	0·8	0·6	[*]	1·0	[1·0]	0·8	0·7	1·0	[0·6]	0·9	1·0	[0·8]	1·0	1·0	0·7

1. Oceanite, Putua, Gambier Isles. [Accumulative.] LACROIX (1927), Anal. 106, p. 45.

2. Labradorite-olivine basalt (β), Mangarera, Gambier Islands. [Accumulative.] LACROIX (1927), Anal. 105, p. 45.

3. Basalt, Nuku-Hiva, Marquesas. [Accumulative.] LACROIX (1927), Anal. 100, p. 42.

4. Labradorite basalt (β), Mangerera, Gambier Islands. LACROIX (1927), Anal. 104, p. 45.

5. Andesine basalt, Taiohoe Bay, Nuku-Hiva, Marquesas. LACROIX (1927), Anal. 99, p. 42.

6. Labradorite andesite, Taiohoe, Nuku-Hiva, Marquesas. LACROIX (1928), Anal. 9, p. 367.

*7. Andesite. Pitcairn Island. LACROIX (1927), Anal. 111, p. 46.

8. Olivine-bearing andesite, Taiohoe, Nuku-Hiva, Marquesas. LACROIX (1928), Anal. 8, p. 367.

*9. Andesite, Pitcairn Island. LACROIX (1927), Anal. 110, p. 46.

10. Biotite andesite, Taiohoe, Nuku-Hiva, Marquesas. LACROIX (1928), Anal. 7, p. 367.

11. Biotite trachyte, Cook Bay, Moorea, Society Islands. LACROIX (1927), Anal. 60, p. 26.

12. Latite, Nuku-Hiva, Marquesas. LACROIX (1927), Anal. 97, p. 42.

*13. Trachyte obsidian, The Rope, Pitcairn Island. LACROIX (1936c), Anal. 6, p. 791.

14. Trachyte, Hua-Huka, Marquesas. LACROIX (1928), Anal. 12, p. 368.

15. Trachyte, Nuku-Hiva, Marquesas. LACROIX (1927), Anal. 95, p. 42.

*16. Trachyte pumice, Pitcairn Island. LACROIX (1936c), Anal. 5, p. 791.

17. Trachyte, Nuku-Hiva, Marquesas. LACROIX (1928), Anal. 3, p. 367.

18. Trachyte, Nuku-Hiva, Marquesas. LACROIX (1927), Anal. 96, p. 42.

19. Trachyte, Nuku-Hiva, Marquesas. LACROIX (1928), Anal. 2, p. 367.

Table 13. *Honolulu Series; Oahu, Hawaiian Islands*

	1	2	3	4	5	6	7	8
Si	$176{\cdot}10^3$	$178{\cdot}10^3$	$175{\cdot}10^3$	$176{\cdot}10^3$	$182{\cdot}10^3$	$201{\cdot}10^3$	$206{\cdot}10^3$	$214{\cdot}10^3$
Al	$63{\cdot}10^3$	$66{\cdot}10^3$	$65{\cdot}10^3$	$60{\cdot}10^3$	$63{\cdot}10^3$	$61{\cdot}10^3$	$67{\cdot}10^3$	$88{\cdot}10^3$
Ti	$17{\cdot}10^3$	$13{\cdot}10^3$	$15{\cdot}10^3$	$18{\cdot}10^3$	$17{\cdot}10^3$	$18{\cdot}10^3$	$14{\cdot}10^3$	$18{\cdot}10^3$
Fe'''	$36{\cdot}10^3$	$37{\cdot}10^3$	$43{\cdot}10^3$	$46{\cdot}10^3$	$37{\cdot}10^3$	$24{\cdot}10^3$	$27{\cdot}10^3$	$24{\cdot}10^3$
Mg	$82{\cdot}10^3$	$78{\cdot}10^3$	$74{\cdot}10^3$	$78{\cdot}10^3$	$79{\cdot}10^3$	$82{\cdot}10^3$	$69{\cdot}10^3$	$34{\cdot}10^3$
Fe''	$65{\cdot}10^3$	$63{\cdot}10^3$	$59{\cdot}10^3$	$58{\cdot}10^3$	$61{\cdot}10^3$	$71{\cdot}10^3$	$72{\cdot}10^3$	$65{\cdot}10^3$
Na	$30{\cdot}10^3$	$39{\cdot}10^3$	$36{\cdot}10^3$	$34{\cdot}10^3$	$32{\cdot}10^3$	$23{\cdot}10^3$	$29{\cdot}10^3$	$27{\cdot}10^3$
Ca	$105{\cdot}10^3$	$97{\cdot}10^3$	$101{\cdot}10^3$	$99{\cdot}10^3$	$93{\cdot}10^3$	$81{\cdot}10^3$	$77{\cdot}10^3$	$82{\cdot}10^3$
K	$5{\cdot}10^3$	$6{\cdot}10^3$	$8{\cdot}10^3$	$10{\cdot}10^3$	$10{\cdot}10^3$	$8{\cdot}10^3$	$8{\cdot}10^3$	$8{\cdot}10^3$
P	(3667)	(6243)	(6288)	(5283)	(4934)	(2271)	(1878)	(2925)
Ga	<5	15	30	10	20	15	20	20
Cr	675	550	450	575	600	500	275	35
V	260	220	150	250	250	225	200	150
Li	10	20	15	20	20	10	7	5
Ni	275	225	175	250	250	325	150	30
Co	60	65	50	70	60	70	40	30
Sc	*	*	*	*	*	*	*	*
Zr	150	120	100	175	120	100	100	100
Mn	(1007)	(852)	(620)	(697)	(852)	(1007)	(697)	(542)
Y	25	25	20	30	25	15	15	15
La	*	*	*	*	*	*	*	*
Sr	1000	2000	2000	2000	2000	1000	750	300
Pb	*	*	*	*	*	*	*	*
Ba	1000	1250	1250	1250	1000	500	650	450
Rb	15	50	50	60	60	50	60	20
Fe	55	56	58	57	55	54	59	72
Mg	45	44	42	43	45	46	41	28
Fe	46	45	46	46	45	46	48	56
Mg	38	35	34	35	36	39	34	22
Alk	16	20	20	19	19	15	18	22
Position	−12·3	−11·0	−10·9	−10·8	−10·1	−8·8	−6·9	−3·7

[Mo, Sn and Cs below their limits of sensitivity in every specimen.]

The accumulative rocks

One accumulative rock of the Hawaiian series and three of the Polynesian series were among the samples available for investigation (Table 11 col. 1; Table 12, cols. 1, 2 and 3). Chromium, nickel and, to a less extent, cobalt are enriched in every case. Vanadium is variable and may be less in amount than that of rocks at the basic end of the liquid line of descent. Lithium, zirconium and yttrium are usually lower than on the liquid line of descent, and this tends to be the case also with strontium and, more especially, barium and rubidium. These features

Table 13*A*. *Honolulu Series; Oahu*

	1	2	3	4	5	6	7	8
Ga × 1000/Al	—	0·23	0·46	0·17	0·32	0·25	0·30	0·23
Cr × 1000/Mg	8·2	7·1	6·1	7·4	7·6	6·1	4·0	1·0
V × 1000/Mg	3·2	2·8	2·0	3·2	3·2	2·7	2·9	4·4
Li × 1000/Mg	0·1	0·3	0·2	0·3	0·3	0·1	0·1	0·1
Ni × 1000/Mg	3·4	2·9	2·4	3·2	3·2	4·0	2·2	0·9
Co × 1000/Mg	0·7	0·8	0·7	0·9	0·8	0·9	0·6	0·9
Fe/Mg	1·2	1·3	1·4	1·3	1·2	1·2	1·4	2·6
Cr × 1000/Fe	6·7	5·5	4·4	5·5	6·1	5·3	2·8	0·4
V × 1000/Fe	2·6	2·2	1·5	2·4	2·6	2·4	2·0	1·7
Co × 1000/Fe	0·6	0·6	0·5	0·7	0·6	0·7	0·4	0·3
Y × 1000/Ca	0·2	0·3	0·2	0·3	0·3	0·2	0·2	0·2
Sr × 100/Ca	1·0	2·1	2·0	2·0	2·2	1·2	1·0	0·4
Sr × 100/Ca + K	0·9	1·9	1·8	1·8	1·9	1·1	0·9	0·3
Ba × 100/K	20	21	16	12·5	10	6·3	8·1	5·6
Rb × 100/K	0·3	0·8	0·6	0·6	0·6	0·6	0·7	0·3

1. Nepheline-melilite basalt, Kaau lava flow, Oahu. WINCHELL (1947), Anal. 16, p. 30.
2. Nepheline-melilite basalt, flow N. of Puu Hawaiiloa, Oahu. WINCHELL (1947), Anal. 20, p. 30.
3. Nepheline-melilite basalt, Haiihi lava flow, Oahu. WINCHELL (1947), Anal. 18, p. 30.
4. Nepheline basalt, Training School flow, Oahu. WINCHELL (1947), Anal. 17, p. 30.
5. Nepheline basalt, lower Nuuanu flow, Oahu. WINCHELL (1947), Anal. 15, p. 30.
6. Nepheline basanite, S. tip of Black Point, Oahu. WINCHELL (1947), Anal. 13, p. 30.
7. Nepheline basanite, Kalama Crater flow, Oahu. WINCHELL (1947), Anal. 14, p. 30.
8. Linosaite, S.W. edge of flow in gulch N. of Hanuama Bay, Oahu. WINCHELL (1947), Anal. 12, p. 30.

are very similar to those already noted in connection with the accumulative rocks of the calc-alkali igneous rock series (NOCKOLDS and ALLEN, 1953, p. 138).

(b) *The Honolulu Series* (*Table* 13)

The Honolulu series comprises a number of highly basic alkaline igneous rocks—nepheline-melilite basalts, nepheline basalts, nepheline basanites, and alkali basalts (linosaites). Three specimens of the first type, two of the second, two of the third, and one of alkali basalt have been investigated for their trace element content. All these, with the exception of the alkali basalt, have features in common. Chromium, nickel and cobalt are present in relatively large amounts, as are strontium and barium. The abundance of the latter, coupled with the low potassium content, leads to very high Ba/K ratios for these rocks (Table 13*A*).

The alkali basalt is similar to that of Papalele Gulch, Hawaii (Table 11, col. 2), but poorer in silicon and richer in sodium. Chromium, vanadium, lithium, nickel, cobalt, zirconium, yttrium and strontium are all lower in amount than in the Papalele rock.

Table 14. *Polynesia; basalt → phonolite series*

	1	2	3	4	5	6	7	8	9	10	11
Si			$213{\cdot}10^3$	$213{\cdot}10^3$	$224{\cdot}10^3$	$225{\cdot}10^3$	$236{\cdot}10^3$	$262{\cdot}10^3$	$262{\cdot}10^3$	$264{\cdot}10^3$	$263{\cdot}10^3$
Al			$61{\cdot}10^3$	$71{\cdot}10^3$	$87{\cdot}10^3$	$107{\cdot}10^3$	$105{\cdot}10^3$	$120{\cdot}10^3$	$120{\cdot}10^3$	$115{\cdot}10^3$	$116{\cdot}10^3$
Ti			$15{\cdot}10^3$	$23{\cdot}10^3$	$17{\cdot}10^3$	$18{\cdot}10^3$	$15{\cdot}10^3$	$12{\cdot}10^2$	$6{\cdot}10^2$	$24{\cdot}10^2$	$36{\cdot}10^2$
Fe'''			$38{\cdot}10^3$	$22{\cdot}10^3$	$41{\cdot}10^3$	$24{\cdot}10^3$	$17{\cdot}10^3$	$17{\cdot}10^3$	$19{\cdot}10^3$	$12{\cdot}10^3$	$31{\cdot}10^3$
Mg			$80{\cdot}10^3$	$50{\cdot}10^3$	$37{\cdot}10^3$	$22{\cdot}10^3$	$9{\cdot}10^3$	$36{\cdot}10^2$	$12{\cdot}10^2$	$10{\cdot}10^2$	$10{\cdot}10^2$
Fe''			$52{\cdot}10^3$	$72{\cdot}10^3$	$33{\cdot}10^3$	$37{\cdot}10^3$	$39{\cdot}10^3$	$47{\cdot}10^2$	$11{\cdot}10^3$	$14{\cdot}10^3$	$19{\cdot}10^2$
Na			$10{\cdot}10^3$	$16{\cdot}10^3$	$19{\cdot}10^3$	$40{\cdot}10^3$	$60{\cdot}10^3$	$80{\cdot}10^3$	$76{\cdot}10^3$	$75{\cdot}10^3$	$54{\cdot}10^3$
Ca			$88{\cdot}10^3$	$85{\cdot}10^3$	$76{\cdot}10^3$	$50{\cdot}10^3$	$46{\cdot}10^3$	$7{\cdot}10^3$	$9{\cdot}10^3$	$10{\cdot}10^3$	$16{\cdot}10^3$
K			$5{\cdot}10^3$	$12{\cdot}10^3$	$21{\cdot}10^3$	$30{\cdot}10^3$	$30{\cdot}10^3$	$42{\cdot}10^3$	$41{\cdot}10^3$	$48{\cdot}10^3$	$54{\cdot}10^3$
P	—	—	(1400)	(2095)	(2185)	(1920)	—	(260)	(310)	(350)	(440)
Ga	10	20	5	25	20	25	25	15	20	15	10
Cr	2500	600	500	300	125	*	*	*	*	*	*
V	250	400	275	280	175	200	250	5	*	*	10
Mo	*	*	*	*	*	10	7	15	10	10	2
Li	2	10	10	15	20	15	35	90	75	65	65
Ni	1500	300	375	320	120	5	*	*	*	*	*
Co	155	75	55	60	30	20	5	*	*	*	*
Sc	*	25	—	—	—	*	*	*	*	*	*
Zr	200	400	175	230	230	500	600	550	700	550	250
Mn	—	—	(1470)	(1240)	(1780)	—	—	(1860)	(2250)	(1470)	(1630)
Y	15	30	20	25	20	40	40	40	50	40	30
La	*	*	*	*	*	100	125	100	175	150	75
Sr	250	1250	800	1000	1800	3000	4000	120	40	40	3000
Pb	*	*	*	*	*	*	*	*	30	30	10
Ba	50	400	400	400	1000	1100	850	30	*	10	2000
Rb	*	30	40	200	275	225	300	1000	1000	950	800
Fe	—	—	53	65	67	73	86	85	97	96	97
Mg	—	—	47	35	33	27	14	15	3	4	3
Fe	—	—	49	55	49	40	36	15	20	17	23
Mg	—	—	43	29	25	14	6	3	1	1	1
Alk	—	—	8	16	26	46	58	82	79	82	76
Position	—	—	−9·2	−5·2	−1·7	+3·3	+5·4	+11·8	+11·8	+12·5	(+12·5)

[Sn and Cs below their limits of sensitivity in every specimen.]

(c) *The Polynesian alkali basalt → phonolite series* (*Table* 14)

The variation diagrams for this series have been drawn on the assumption that the parental magma is the same as that of the Polynesian alkali basalt → trachyte series (Table 12, col. 4).

Silicon and Oxygen (*Fig.* 26*d*). The curves for silicon and oxygen rise less steeply than in the alkali basalt → trachyte series, the ratio of Si : O ranging from 1 : 2 at the basic end to 1 : 1·7 at the acid end of the series.

Aluminium and Gallium (*Fig.* 26*d*). The curve for aluminium rises more or less steadily as the function $[(\frac{1}{3}\mathrm{Si} + \mathrm{K}) - (\mathrm{Ca} + \mathrm{Mg})]$ increases, but the curve for gallium remains practically horizontal throughout. As a result, there is increasing divergence between the two curves, and the Ga/Al ratio decreases as the late-stage members of the series are reached (Table 14*A*). The average ratio, for what it is worth, of Ga × 1000/Al is 0·21.

Table 14*A*. *Polynesia; basalt → phonolite series*

	3	4	5	6	7	8	9	10	11
Ga × 1000/Al	0·1	0·35	0·23	0·23	0·24	0·13	0·17	0·13	0·09
Cr × 1000/Mg	6·2	6·0	3·4	*	*	*	*	*	*
V × 1000/Mg	3·4	5·6	4·7	9·1	2·8	1·4	*	*	10
Li × 1000/Mg	0·1	0·3	0·5	0·7	3·9	25	62	65	65
Ni × 1000/Mg	4·7	6·4	3·2	0·2	*	*	*	*	*
Co × 1000/Mg	0·7	1·2	0·8	0·9	0·6	*	*	*	*
Fe/Mg	1·1	1·9	2·0	2·8	6·2	6·0	25	26	33
Cr × 1000/Fe	5·6	3·2	1·7	*	*	0·05	*	*	*
V × 1000/Fe	3·1	3·0	2·4	3·3	4·5	0·2	*	*	0·3
Co × 1000/Fe	0·6	0·6	0·4	0·3	0·1	*	*	*	*
Y × 1000/Ca	0·2	0·3	0·3	0·8	0·9	5·7	5·6	4·0	1·9
Sr × 100/Ca	0·9	1·2	2·4	6·0	8·7	1·7	0·4	0·4	18·7
Sr × 100/Ca + K	0·9	1·0	1·9	3·7	5·3	0·2	0·1	0·1	4·3
Ba × 100/K	8·0	3·3	4·8	3·7	2·8	0·1	*	0·02	3·7
Rb × 100/K	0·8	1·7	1·3	0·8	1·0	2·4	2·4	2·0	1·5

1. Oceanite, Tahiti, Society Is. [Accumulative.]
2. Ankaramite, Papeeti, Tahiti, Society Is. [Accumulative.]
3. Ankaramitic basalt, Ua Huka Isle, Marquesas. [Accumulative.] LACROIX (1928), Anal. 15, p. 368.
4. Labradorite basalt (β), Ua Pou Isle, Marquesas. LACROIX (1931), Anal. 2, p. 1166.
5. Basalt, Hikea, Ua Pou Isle, Marquesas. LACROIX (1928), Anal. 16, p. 368.
6. Essexite, Tahiti, Society Is. LACROIX (1927), Anal. 6, p. 8.
7. Tahitite, Tahiti, Society Is. LACROIX (1927), Anal. 38, p. 18.
8. Aegirine-nepheline phonolite, Hakaketou, Ua Pou Isle, Marquesas. LACROIX (1931), Anal. 1, p. 1161.
9. Phonolite, Pautetainui, Ua Pou Isle, Marquesas. LACROIX (1931), Anal. 2, p. 1161.
10. Aegirine phonolite, Paumaka, Ua Pou Isle, Marquesas. LACROIX (1931), Anal. 4, p. 1161.
11. Leucite phonolite, Ua Pou Isle, Marquesas. LACROIX (1931), Anal. 6, p. 1161.

Magnesium, *Nickel*, *Lithium*, *Iron*, *Cobalt*, *Chromium*, *Vanadium*, *Titanium* (*Fig.* 27*d*). As usual, magnesium shows a steady decrease as the function $[(\frac{1}{3}\text{Si} + \text{K}) - (\text{Ca} + \text{Mg})]$ increases and, in this series, iron does the same. Chromium and nickel both decline rapidly and fall below their limits of sensitivity at about the same time. Cobalt remains more or less constant for a time and then gradually declines. Once more this results in early rocks having Ni > Co, and later ones having Ni < Co. Titanium behaves here rather like cobalt, but declines more gradually.

In spite of the fact that iron declines steadily, vanadium increases in amount in the intermediate members of the series and then declines sharply. The vanadium curve has thus a pronounced maximum which lies at a higher value for the function $[(\frac{1}{3}\text{Si} + \text{K}) - (\text{Ca} + \text{Mg})]$ than the maxima on the vanadium curves for the Hawaiian, Polynesia and Scottish Tertiary alkali basalt → trachyte series.

Lithium increases steadily, and more markedly than in the basalt → trachyte series, as the function $[(\frac{1}{3}\text{Si} + \text{K}) - (\text{Ca} + \text{Mg})]$ rises in value.

The ratios Cr/Mg, Cr/Fe, Ni/Mg, Co/Mg and Co/Fe all show a progressive decrease on passing from early basic to late-stage members of the series. The ratio Li/Mg shows a marked increase in the same direction, while the ratio V/Fe passes through a maximum in the intermediate stages.

Fig. 28*a–g*. Variation in calcium, strontium, barium, sodium, rubidium and potassium. Values in weight per cent, Sr, Ba and Rb × 100.

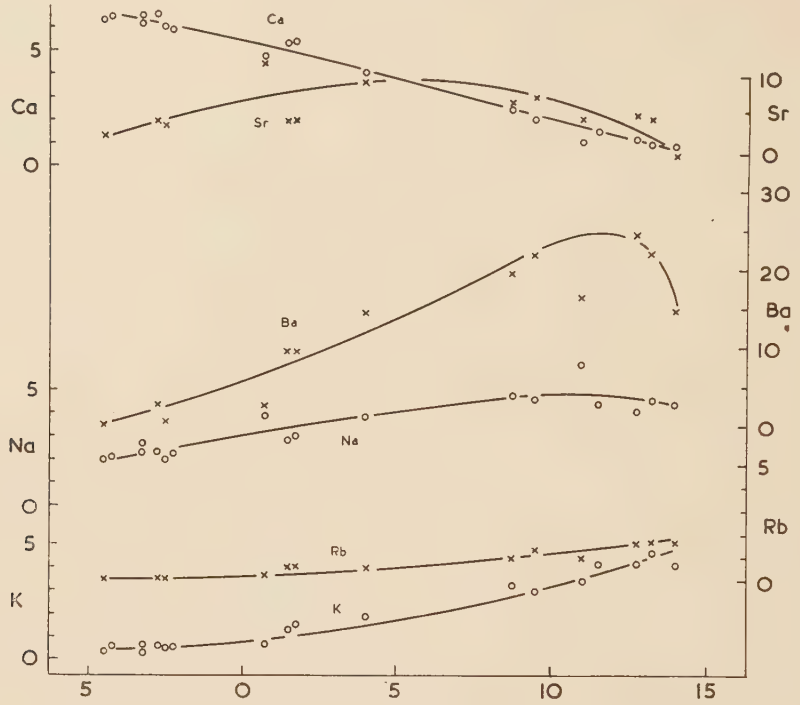

Fig. 28*a*. Scottish Tertiary alkali basalt → trachyte series.

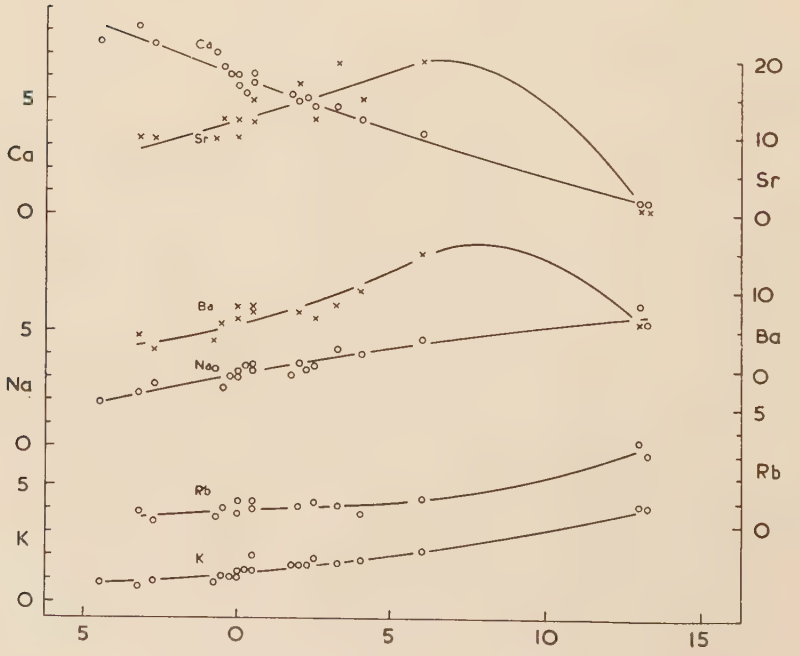

Fig. 28*b*. Hawaiian alkali basalt → trachyte series.

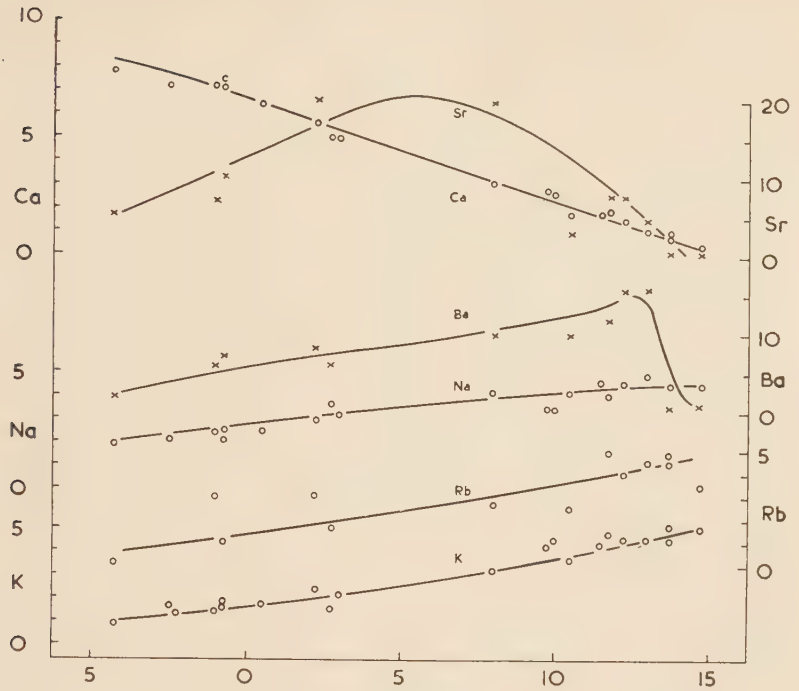

Fig. 28c. Polynesian alkali basalt → trachyte series.

Calcium and Strontium (*Fig.* 28*d*). Calcium decreases slowly at first, and then more rapidly, as the function $[(\frac{1}{3}\text{Si} + \text{K}) - (\text{Ca} + \text{Mg})]$ increases. When the more rapid decline sets in, the curve becomes virtually linear. Strontium is markedly enriched in the rocks of this series so far as the basic and intermediate types are concerned, but the end-stage members are almost devoid of that element. Thus, just as in the alkali basalt → trachyte series, the strontium curve passes through a maximum which is here exceptionally pronounced, owing to the high Sr content of the intermediate members.

The ratios Sr/Ca and Sr/Ca + K both pass through a maximum at the intermediate stage and fall to very low values when the end-stage members are reached.

Yttrium. Yttrium increases in amount on passing from the early basic to the intermediate members of the series but, after this, remains more or less constant. But as Ca is declining throughout, the ratio Y/Ca shows a marked increase in the late-stage members.

Lanthanum. Lanthanum rise above the limit of sensitivity in the intermediate members of the series, and from then on tends to increase slightly.

Sodium (*Fig.* 28*d*). Sodium increases steadily and sharply in this series as the value of the function $[(\frac{1}{3}\text{Si} + \text{K}) - (\text{Ca} + \text{Mg})]$ increases, and this continues into the latest stages. As a result there is a marked concentration of Na in late-stage members here as compared with the corresponding members of the alkali basalt → trachyte series.

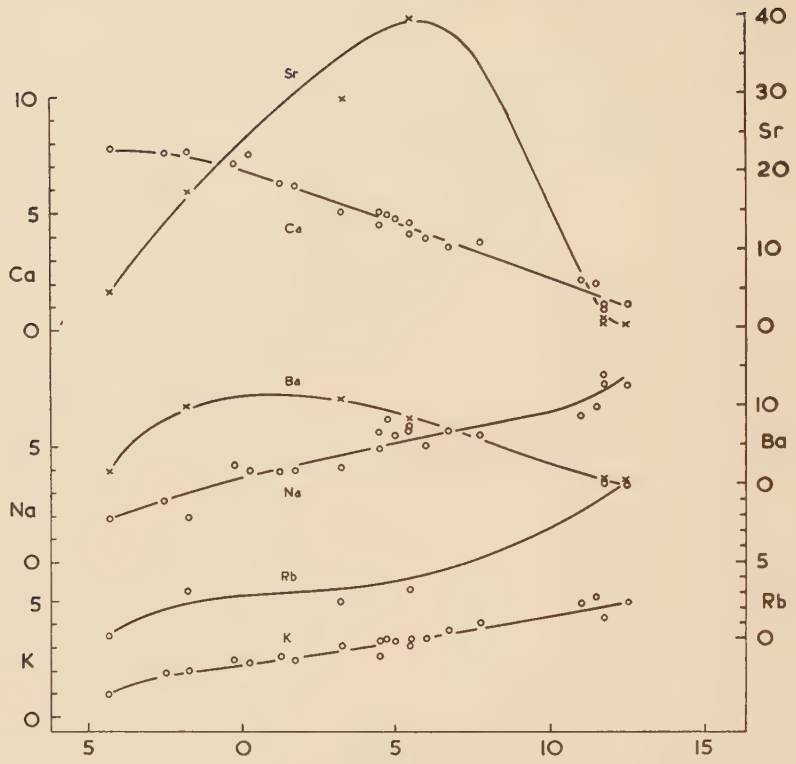

Fig. 28*d*. Polynesian alkali basalt → phonolite series.

Potassium, Barium, Rubidium, Caesium, Lead (*Fig.* 28*d*). Potassium shows a steady rise as the value of the function $[(\frac{1}{3}\text{Si} + \text{K}) - (\text{Ca} + \text{Mg})]$ increases. Barium is not enriched to anything like the same extent as strontium, and such enrichment as does occur takes place at an early intermediate stage. The curve for Ba thus passes through a feeble maximum at a lower value of the function $[(\frac{1}{3}\text{Si} + \text{K}) - (\text{Ca} + \text{Mg})]$ than the maximum for Sr and thereafter declines steadily. As in the case of Sr, the late-stage members of the series are virtually devoid of Ba. The Ba/K ratio does not change much in the basic and intermediate members of the series but falls to a very low value in the late-stage members.

We have already seen that normally, in both calc-alkali igneous rock series and in alkali basalt → trachyte series, the curve for rubidium is almost parallel with that of potassium, at any rate until a very late stage. The present series is somewhat different in this respect. The two curves remain parallel for some time as the value of the function $[(\frac{1}{3}\text{Si} + \text{K}) - (\text{Ca} + \text{Mg})]$ increases but the increase

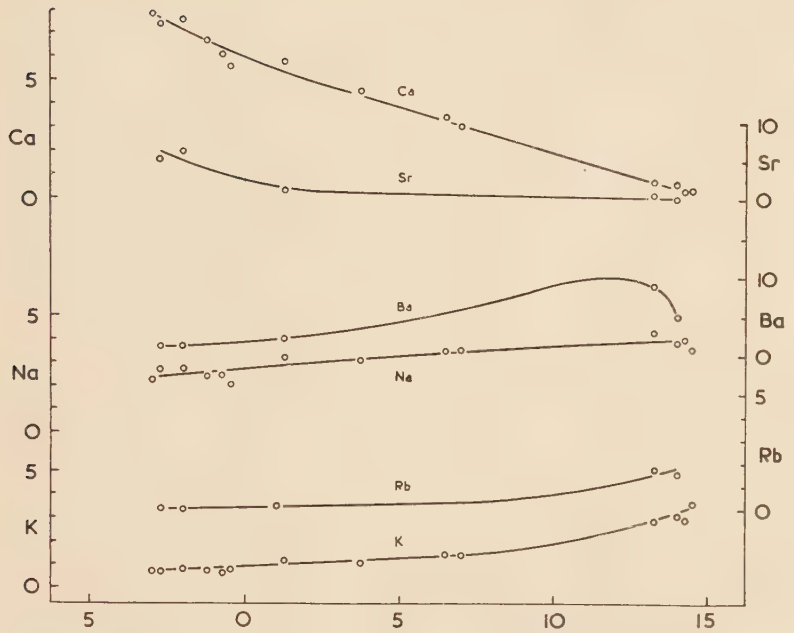

Fig. 28*e*. Easter Island basalt → alkali rhyolite series.

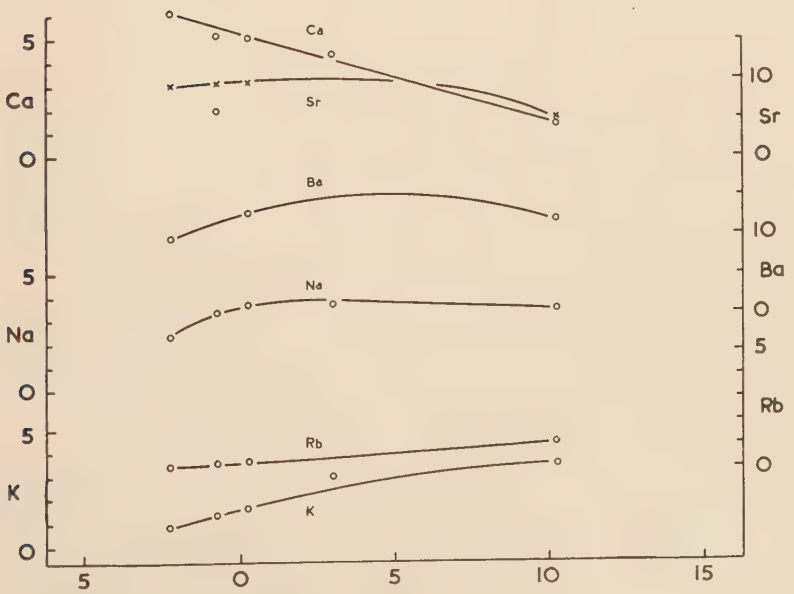

Fig. 28*f*. Braefoot Outer Sill.

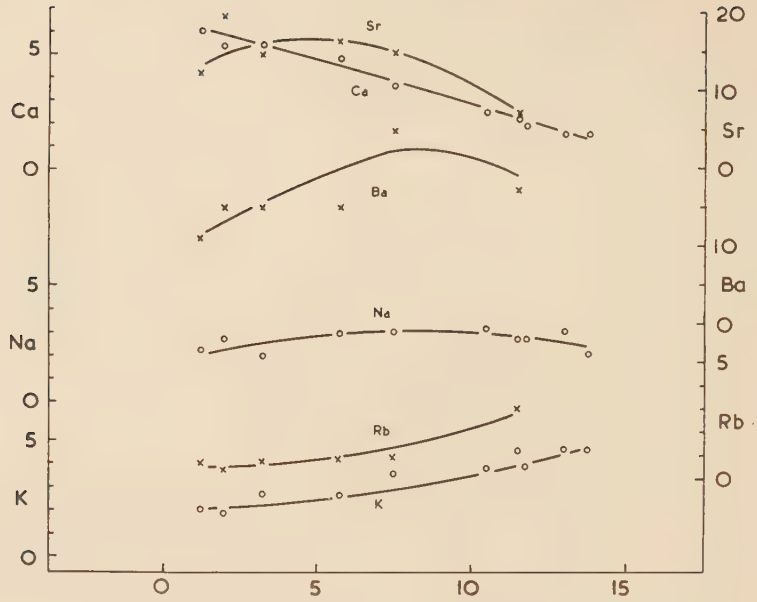

Fig. 28*g*. E. Central Sierra Nevada latite series.

in Rb in the later stages leads then to a marked divergence. The Rb/K ratio is higher than usual throughout practically the whole series, and Rb $\times$ 100/K is $>2{\cdot}0$ in the late-stage members where Rb is concentrated to the extent of 1000 ppm or more.

Caesium has not been found to rise above its limit of sensitivity in any rock of the series, despite the high rubidium content of some.

Lead is below the limit of sensitivity throughout most of the series, appearing in small amounts only in the extreme late-stage members.

Zirconium (*Fig.* 29). Zirconium increases rapidly in amount until the early intermediate members of the series are reached, after which it appears to remain more or less constant.

Molybdenum. Molybdenum behaves much like zirconium in the sense that it appears in appreciable amounts in the early intermediate members of the series and thereafter remains more or less constant.

It will be observed that the leucite-phonolite associated with the normal phonolites of this series (Table 14, col. 11) does not fit the variation diagram for the series. Its trace element content, too, differs from that of the normal phonolites.

The accumulative rocks

Four accumulative rocks of this series have been investigated, two of which have been analysed for their major constituents. All show a concentration of chromium, nickel, cobalt and vanadium, with impoverishment in strontium, barium, rubidium, and lithium when compared with rocks lying on the liquid line of descent. They thus behave in the same kind of way as the accumulative rocks of other igneous rock series.

Table 15. *Polynesia: Easter Islands; basalt → obsidian series*

	1	2	3	4	5
Si	$219 \cdot 10^3$	$231 \cdot 10^3$	$238 \cdot 10^3$	$337 \cdot 10^3$	$348 \cdot 10^3$
Al	$77 \cdot 10^3$	$71 \cdot 10^3$	$83 \cdot 10^3$	$73 \cdot 10^3$	$66 \cdot 10^3$
Ti	$25 \cdot 10^3$	$23 \cdot 10^3$	$14 \cdot 10^3$	$2 \cdot 10^3$	$6 \cdot 10^2$
Fe‴	$73 \cdot 10^3$	$15 \cdot 10^3$	$13 \cdot 10^3$	$4 \cdot 10^3$	$3 \cdot 10^3$
Mg	$34 \cdot 10^3$	$29 \cdot 10^3$	$20 \cdot 10^3$	$4 \cdot 10^2$	tr.
Fe″	$22 \cdot 10^3$	$80 \cdot 10^3$	$86 \cdot 10^3$	$21 \cdot 10^3$	$19 \cdot 10^3$
Na	$27 \cdot 10^3$	$27 \cdot 10^3$	$33 \cdot 10^3$	$44 \cdot 10^3$	$39 \cdot 10^3$
Ca	$74 \cdot 10^3$	$76 \cdot 10^3$	$59 \cdot 10^3$	$8 \cdot 10^3$	$7 \cdot 10^3$
K	$7 \cdot 10^3$	$8 \cdot 10^3$	$12 \cdot 10^3$	$28 \cdot 10^3$	$31 \cdot 10^3$
P	(1965)	(2050)	(1750)	—	—
Ga	20	20	20	20	30
Cr	80	50	*	*	*
V	400	400	30	*	*
Mo	*	*	*	5	10
Li	10	10	15	65	65
Ni	50	30	*	*	*
Co	50	35	*	*	*
Sc	—	—	—	—	—
Zr	350	300	250	650	750
Mn	(775)	(1470)	(1500)	(850)	(465)
Y	40	40	45	70	100
La	*	*	*	100	150
Sr	500	600	100	30	*
Pb	*	*	*	10	15
Ba	100	100	200	900	500
Rb	*	*	10	175	150
Fe	74	77	83	98	99+
Mg	26	23	17	2	1−
Fe	58	60	61	25	24
Mg	21	18	12	0·5	tr.
Alk	21	22	27	74·5	76
Position	−2·8	−2·0	+1·2	+13·2	+14·0

[Sn and Cs below their limits of sensitivity in every specimen.]

Table 15*A*. *Easter Islands; basalt → obsidian series*

	1	2	3	4	5
Ga × 1000/Al	0·26	0·28	0·24	0·27	0·45
Cr × 1000/Mg	2·4	1·7	*	*	*
V × 1000/Mg	11·8	13·8	1·5	*	*
Li × 1000/Mg	0·3	0·3	0·75	162	>650
Ni × 1000/Mg	1·5	1·0	*	*	*
Co × 1000/Mg	1·5	1·2	*	*	*
Fe/Mg	2·8	3·3	4·9	62	>220
Cr × 1000/Fe	0·8	0·5	*	*	*
V × 1000/Fe	4·2	4·2	0·3	*	*
Co × 1000/Fe	0·5	0·4	*	*	*
Y × 1000/Ca	0·5	0·5	0·8	8·7	14·3
Sr × 100/Ca	0·7	0·8	0·2	0·4	*
Sr × 100/Ca + K	0·6	0·7	0·1	0·1	*
Ba × 100/K	1·4	1·3	1·7	3·2	1·6
Rb × 100/K	*	*	0·1	0·6	0·5

1. Basalt (β) scoriae, Ankena. LACROIX (1936b), Anal. 1, p. 602.

2. Aphyric basalt (β), Aho Tongariki. LACROIX (1936b), Anal. 3, p. 602.

3. Aphyric basalt (β), Rano Roraku. LACROIX (1936b), Anal. 2, p. 602.

4. Rhyolite obsidian, Mt. Orito. LACROIX (1936b), Anal. 13, p. 603.

5. Rhyolite obsidian, Ranohao. LACROIX (1936b), Anal. 12, p. 603.

(d) *The Easter Island basalt → obsidian series* (*Table* 15)

We have, unfortunately, only a few of the analyzed specimens from this island available for trace element determinations, but the curves given for the various trace elements are believed to be approximately correct. The series is very different from the other alkali series and the supposed parental magma (Table 17) has a higher Fe/Mg ratio than the others. In harmony with this, the chromium and nickel contents are lower, and the vanadium and cobalt contents higher, than in the other supposed parental magmas.

Silicon and Oxygen (*Fig.* 26*e*). The ratio of Si : O ranges from 1 : 2 at the basic end to 1 : 1·4 at the acid end of the series. The upward rise of the Si curve is relatively sharp and reflects the high silicon content of the late-stage members of the series.

Aluminium and Gallium (*Fig.* 26*e*). The curve for aluminium remains almost unchanged for a time and then declines slowly, but definitely, as the value of the function $[(\frac{1}{3}\mathrm{Si} + \mathrm{K}) - (\mathrm{Ca} + \mathrm{Mg})]$ increases. The curve for gallium, on the other hand, rises slightly in the same direction with the result that we have here an increase in the Ga/Al ratio at the extreme acid end of the series. The average Ga × 1000/Al for the series is 0·30.

Magnesium, Nickel, Lithium, Iron, Cobalt, Chromium, Vanadium, Titanium (*Fig.* 27*e*). Magnesium decreases steadily as the value of the function [($\frac{1}{3}$Si + K) − (Ca + Mg)] rises. Chromium, nickel, cobalt and vanadium are all rapidly eliminated and soon fall below their limits of sensitivity. It is interesting to find that vanadium, which is enriched in the supposed parental magma, is eliminated as rapidly as the other trace elements. In fact all four of them fall below their limits of sensitivity at about the same time. Moreover, as in the case of certain calc-alkali igneous rock series, the higher Fe/Mg ratio of the parental magma leads to the latter having a higher Co/Ni ratio, which is here unity. As Co decreases slightly less rapidly than Ni, the cobalt curve lies above the nickel curve until both elements fall below their limit of sensitivity.

The curve for iron passes through a maximum near the basic end of the series, but there is apparently no corresponding maximum on the curve for vanadium.

Lithium increases steadily, and quite markedly, in amount as we pass from the basic to the acid end of the series, and there is consequently a great increase in the Li/Mg ratio in this direction (Table 15*A*). Titanium decreases steadily in the same direction.

Thus this group of elements, taken as a whole, shows considerable difference of behaviour when compared with the same group in the other alkali series.

Calcium and Strontium (*Fig.* 28*e*). Calcium shows a virtually linear decrease in amount as the value of the function [($\frac{1}{3}$Si + K) − (Ca + Mg)] increases. Strontium, unlike its behaviour in the other alkali series, is soon almost eliminated and falls to about 100 ppm, after which it continues to decline more slowly. As a result, the ratios Sr/Ca and Sr/Ca + K both decline rapidly.

Yttrium. Yttrium is present in appreciable amounts throughout but is here definitely concentrated in the late-stage members of the series where the ratio Y/Ca is, as a consequence, much enhanced (Table 15*A*).

Lanthanum. Lanthanum is below its limit of sensitivity at the basic end of the series but, like Y, appears to be concentrated to some extent in the late-stage members.

Sodium (*Fig.* 28*e*). Sodium increases steadily as the value of the function [($\frac{1}{3}$Si + K) − (Ca + Mg)] rises and this continues even in the extreme late-stage members of the series. The slope of the curve is gentle and the sodium content is about doubled on passing from the basic to the extreme late-stage members.

Potassium, Barium, Rubidium, Caesium, Lead (*Fig.* 28*e*). Potassium increases slowly at first but the curve for K steepens as we pass from the intermediate to the late-stage members of the series, and in the latter the values for K approach those for Na though, with one exception, K remains lower than Na.

Barium behaves here as it does in some calc-alkali igneous rock series and in the alkali basalt → trachyte series, that is, it reaches its maximum value near the extreme late-stage members and then declines very rapidly as the latter are reached. The values for Ba are, however, never very great, the maximum attained being about 1000 ppm. The supposed parental magma is poor in Ba and this maximum represents a ten-fold increase.

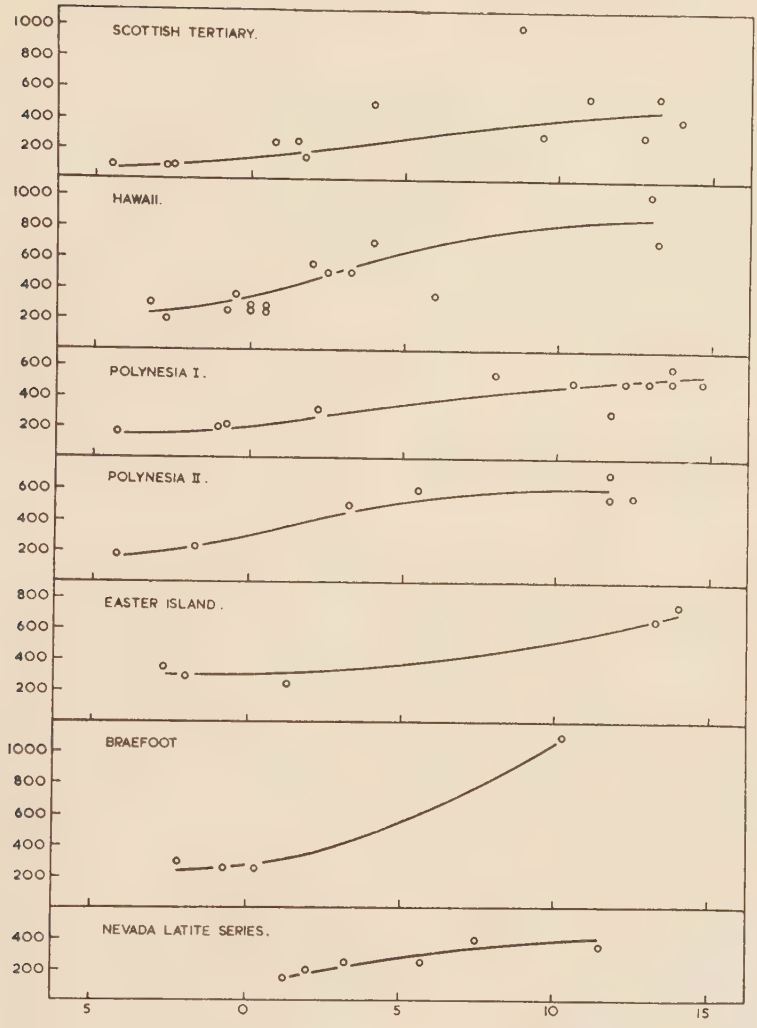

Fig. 29. Variation in zirconium. Values in ppm.

Rubidium is below the limit of sensitivity in the basic members of this series but has a value of some 150 ppm in the late-stage members. We have no intermediate points to guide us but it is likely that the curve for Rb will be parallel with that for K, as it is in so many other igneous rock series.

Caesium has not been found above its limit of sensitivity and lead appears in small amounts only in the late-stage members.

We have had no accumulative rocks of this series available for investigation.

Table 16. *E. Central Sierra Nevada; latite series*

	1	2	3	4	5	6	7	8	9	10
Si	$248{\cdot}10^3$	$258{\cdot}10^3$	$254{\cdot}10^3$	$265{\cdot}10^3$	$265{\cdot}10^3$	$297{\cdot}10^3$	$224{\cdot}10^3$	$230{\cdot}10^3$	$251{\cdot}10^3$	$236{\cdot}10^3$
Al	$97{\cdot}10^3$	$91{\cdot}10^3$	$97{\cdot}10^3$	$102{\cdot}10^3$	$97{\cdot}10^3$	$93{\cdot}10^3$	$86{\cdot}10^3$	$81{\cdot}10^3$	$97{\cdot}10^3$	$91{\cdot}10^3$
Ti	$6{\cdot}10^3$	$5{\cdot}10^3$	$6{\cdot}10^3$	$7{\cdot}10^3$	$11{\cdot}10^3$	$7{\cdot}10^3$	$7{\cdot}10^3$	$6{\cdot}10^3$	$6{\cdot}10^3$	$8{\cdot}10^3$
Fe'''	$17{\cdot}10^3$	$31{\cdot}10^3$	$15{\cdot}10^3$	$33{\cdot}10^3$	$22{\cdot}10^3$	$9{\cdot}10^3$	$9{\cdot}10^3$	$13{\cdot}10^3$	$24{\cdot}10^3$	$41{\cdot}10^3$
Mg	$31{\cdot}10^3$	$32{\cdot}10^3$	$25{\cdot}10^3$	$9{\cdot}10^3$	$12{\cdot}10^3$	$8{\cdot}10^3$	$68{\cdot}10^3$	$65{\cdot}10^3$	$34{\cdot}10^3$	$43{\cdot}10^3$
Fe''	$42{\cdot}10^3$	$26{\cdot}10^3$	$47{\cdot}10^3$	$18{\cdot}10^3$	$29{\cdot}10^3$	$22{\cdot}10^3$	$64{\cdot}10^3$	$54{\cdot}10^3$	$37{\cdot}10^3$	$40{\cdot}10^3$
Na	$22{\cdot}10^3$	$27{\cdot}10^3$	$19{\cdot}10^3$	$29{\cdot}10^3$	$30{\cdot}10^3$	$27{\cdot}10^3$	$19{\cdot}10^3$	$18{\cdot}10^3$	$21{\cdot}10^3$	$19{\cdot}10^3$
Ca	$60{\cdot}10^3$	$53{\cdot}10^3$	$54{\cdot}10^3$	$48{\cdot}10^3$	$36{\cdot}10^3$	$21{\cdot}10^3$	$69{\cdot}10^3$	$70{\cdot}10^3$	$62{\cdot}10^3$	$65{\cdot}10^3$
K	$20{\cdot}10^3$	$18{\cdot}10^3$	$27{\cdot}10^3$	$27{\cdot}10^3$	$35{\cdot}10^3$	$45{\cdot}10^3$	$8{\cdot}10^3$	$17{\cdot}10^3$	$11{\cdot}10^3$	$6{\cdot}10^3$
P	(1529)	(1529)	—	(1922)	(2795)	(306)	(2227)	(1790)	(2227)	—
Ga	30	30	30	30	30	25	25	20	30	25
Cr	100	200	55	60	10	*	450	1000	800	200
V	200	200	200	200	250	70	300	300	250	150
Mo	*	*	3	5	5	3	*	*	*	*
Li	25	20	15	25	25	20	25	20	10	10
Ni	40	85	35	35	25	*	150	300	100	125
Co	20	30	25	35	20	*	35	50	35	30
Sc	*	*	*	*	*	*	*	30	30	*
Zr	150	200	250	250	400	350	150	150	150	100
Mn	(1859)	(1162)	—	(1007)	(1240)	(930)	(1781)	(1704)	(542)	—
Y	20	20	25	40	50	30	20	20	20	20
La	*	*	*	75	75	100	*	*	*	*
Sr	1250	2000	1500	1650	1500	650	2350	2000	1000	300
Pb	*	15	15	20	30	40	*	*	10	*
Ba	1100	1500	1500	1500	2500	1700	1000	2000	1000	350
Rb	70	40	80	80	80	300	100	60	10	10
Cs	*	*	*	*	*	15	*	*	*	*
Fe	66	64	71	85	81	79	52	51	64	65
Mg	34	36	29	15	19	21	48	49	36	35
Fe	45	42	46	44	40	28	44	40	48	54
Mg	23	24	19	8	9	7	40	39	27	29
Alk	32	34	35	48	51	65	16	21	25	17
Position	+1·2	+1·9	+3·3	+5·8	+7·5	+11·5	−5·4	−4·1	−0·1	−2·3

[Sn below its limit of sensitivity in every specimen.]

(e) *The Braefoot Sill* (*Figs.* 26*f*, 27*f*, 28*f* and 29).

The figures and the comments that follow are based on the values given by Higazy (Higazy, 1952).

There is a sharp rise in the curves for Si and O at the acid end and this is coupled with a decrease of aluminium, while gallium tends to rise in the same direction. There is thus some increase in the Ga/Al ratio.

Table 16A. E. Central Sierra Nevada; latite series

	1	2	3	4	5	6	7	8	9	10
Ga × 1000/Al	0·31	0·33	0·31	0·29	0·31	0·27	0·29	0·25	0·31	0·27
Cr × 1000/Mg	3·2	6·2	2·2	6·7	0·8	*	6·6	15·4	24	4·7
V × 1000/Mg	6·5	6·2	8·0	2·2	2·1	8·8	4·4	4·6	7·4	3·5
Li × 1000/Mg	0·8	0·6	0·6	2·8	2·1	2·5	0·4	0·3	0·3	0·2
Ni × 1000/Mg	1·3	2·7	1·4	3·9	2·1	*	2·2	4·6	2·9	2·9
Co × 1000/Mg	0·6	0·9	1·0	3·9	1·7	*	0·5	0·8	1·0	0·7
Fe/Mg	1·9	1·8	2·5	5·7	4·3	3·9	1·1	1·0	1·8	1·9
Cr × 1000/Fe	1·7	3·8	0·9	1·2	0·2	*	6·2	15	13	2·5
V × 1000/Fe	3·4	3·8	3·2	3·9	4·9	2·3	4·1	4·5	4·1	1·9
Co × 1000/Fe	0·3	0·5	0·4	0·7	0·5	*	0·5	0·7	0·6	0·4
Y × 1000/Ca	0·3	0·4	0·5	0·8	1·4	1·4	0·3	0·3	0·3	0·3
Sr × 100/Ca	2·1	3·8	2·7	3·4	4·2	3·1	3·4	2·9	1·6	0·5
Sr × 100/Ca + K	1·6	2·8	1·9	2·2	2·1	1·0	3·1	2·3	1·4	0·4
Ba × 100/K	5·5	8·3	5·6	5·6	7·1	3·8	12·5	11·8	9·1	5·8
Rb × 100/K	0·3	0·2	0·3	0·3	0·2	0·7	1·2	0·4	0·1	0·2

1. Basalt (Pliocene), Mill Creek, Bridgeport quadrangle. (HALSEY, No. 42.)
2. Basaltic pyroxene andesite, flow at base of latite series, West Walker River Canyon. (HALSEY, No. 57A.) [This rock is unduly high in Cr and Ni.]
3. Basaltic andesite. (HALSEY, No. V, B.)
4. Porphyritic latite, second flow above No. 57A. (HALSEY, No. 57E.)
5. Non-porphyritic latite, flow above No. 57E. (HALSEY, No. 57F.)
6. Glassy inclusion from latite welded-tuff-breccia, on ridge 3 miles W. of Sonora Pass, Dardanelles quadrangle (SLEMMONS, No. 892.)
7. Olivine basalt (? late Pliocene), flow W. of Sonora Pass, Dardanelles quadrangle. (SLEMMONS, No. 22.)
8. Olivine basalt (late Pliocene), flow above West Walker River, Bridgeport quadrangle. (HALSEY, No. 812.)
9. Olivine basalt (pre-latite; Miocene-Pliocene), ? flow, near Sonora Junction, Bridgeport quadrangle. (HALSEY, No. 72.)
10. Post-andesite olivine basalt flow. (HALSEY, No. 44-I-11). [Possible parent of both series.]

Chromium, nickel and cobalt have high values in the more basic rocks and the scale for the Cr curve is here one-fifth of that used in the other figures while nickel and cobalt are also shown on a reduced scale. Nickel decreases rapidly at first, then less so, and it never falls below the curve for cobalt as it does in all the other rock series dealt with in this paper so far. Iron falls steadily but, in spite of this, vanadium has a gentle maximum near the basic end of the series.

Calcium decreases in linear fashion, strontium and barium both probably pass through a feeble maximum, as does sodium. Potassium rises steadily at first, then more slowly. Rubidium rises gently throughout, and the curves for potassium and rubidium converge as the value of the function $[(\frac{1}{3}\text{Si} + \text{K}) - (\text{Ca} + \text{Mg})]$ increases.

(f) *The East Central Sierra Nevada basalt → latite series* (*Table* 16)

This is a series of quite different character from those already described, and in which the main feature is richness in potassium rather than sodium.

Table 17. *Approximate chemical composition of some parental magmas of alkali series*

	1	2	3	4	5	6	7	8	9
SiO_2	46·1	46·7	46·0	45·3	45·8	48·2	47·5	47·2	53·2
TiO_2	2·5	3·0	2·9	2·2	2·3	2·4	3·0	4·9	1·0
Al_2O_3	15·1	15·3	16·9	15·3	16·6	15·9	15·7	15·1	18·3
Fe_2O_3	3·0	3·8	4·6	3·0	4·6	3·6	4·2	4·1	2·5
FeO	10·4	8·2	7·4	10·2	8·6	9·3	8·3	8·2	5·4
MnO	0·23	0·10	0·18	0·20	0·11	0·2	0·20	0·15	0·24
MgO	10·4	8·5	7·3	8·7	7·9	7·4	6·2	5·0	5·2
CaO	9·3	10·5	10·9	11·2	8·4	8·6	10·4	11·1	8·4
Na_2O	2·5	2·6	2·5	3·0	3·8	3·1	3·0	2·9	3·0
K_2O	0·3	1·0	1·0	0·6	1·2	1·0	1·1	0·8	2·4
P_2O_5	0·22	0·33	0·26	0·29	0·71	0·3	0·42	0·50	0·35
Fe	62	64	67	66	68	69	72	76	66
Mg	38	36	33	34	32	31	28	24	34

1. Scottish Tertiary basalt → trachyte series [average of basalts from Fishnish, Mull and Morven; and crinanite from Jura]. (These rocks are somewhat altered.)

2. Hawaiian basalt → trachyte series [aphyric basalt, Maunakea; Macdonald (1949), Anal. 1, p. 83].

3. Polynesian basalt → trachyte and basalt → phonolite series [basalt, Gambier Is.; Lacroix (1927), Anal. 104, p. 45].

4. Younger basalt of Later Series, Mauritius [average of four analyses]. (Data kindly supplied by Prof. F. Walker.)

5. Rocks of the Circular Head Laccolith, Tasmania [chilled base of Laccolith; Edwards (1941), Anal. 1, p. 407].

6. Braefoot Outer Sill [basalt near base of sill; Campbell, Day and Stenhouse (1933), Anal. 1, p. 349]. (This rock is somewhat altered.)

7. Mauritius basalt → trachyte series (Old Series) [average of basalts Nos. 350 and 275]. (Data kindly supplied by Prof. F. Walker.)

8. Easter Island basalt → obsidian series [basalt; Lacroix (1936b), Anal. 5, p. 602].

9. E. Central Sierra Nevada Latite Series latitic basalt (Halsey, No. 42)].

Silicon and Oxygen (*Fig.* 26*g*). Both show a steady rise throughout the series, the Si : O ratio varying from 1 : 1·8 at the basic end to 1 : 1·5 at the acid end.

Aluminium and Gallium (*Fig.* 26*g*). The curve for aluminium passes through a feeble maximum and then declines a little as the function $[(\frac{1}{3}\text{Si} + \text{K}) - (\text{Ca} + \text{Mg})]$ increases in value. The curve for Ga follows that for Al, the ratio Ga × 1000/Al being practically constant throughout the range covered by our specimens (Table 16*A*), and averaging 0·30.

Magnesium, Nickel, Lithium, Iron, Cobalt, Chromium, Vanadium, Titanium (*Fig.* 27*g*). Magnesium and chromium decrease steadily as the function $[(\frac{1}{3}\text{Si} + \text{K}) - (\text{Ca} + \text{Mg})]$ rises in value and chromium eventually falls below the limit of sensitivity. Nickel lies above cobalt, until they both fall below the limit of sensitivity at about the same time as Cr. The curves for Ni and Co approach more and more closely, however, because Co decreases at first less rapidly than Ni. Iron also decreases slowly and the Co curve is nearly parallel with the Fe curve throughout much of its range. Vanadium remains practically constant for a time and then declines sharply. Lithium is virtually constant throughout the range covered by our specimens. Titanium, too, shows little change.

The ratios Cr/Mg, V/Mg and, more surprisingly, Ni/Mg and Co/Mg are all rather capricious, but the ratio Li/Mg increases as the value of the function $[(\frac{1}{3}\text{Si} + \text{K}) - (\text{Ca} + \text{Mg})]$ increases. As would be expected from the form of the

Fig. 30. Diagram showing variation in composition of parental magmas. (Numbers refer to analysis in Table 17.)

curves for the elements concerned, the ratio Cr/Fe decreases (except for No. 2 which is exceptionally rich in Cr), while the ratio V/Fe remains more or less constant until specimen No. 6, when it decreases. The ratio Co/Fe also shows little change as far as it can be followed, and Co $\times$ 1000/Fe averages 0·5.

Calcium and Strontium (*Fig.* 28*g*). Calcium shows a linear decrease with increase in the value of the function $[(\frac{1}{3}\text{Si} + \text{K}) - (\text{Ca} + \text{Mg})]$, but strontium has a maximum towards the basic end of the series and then declines. The ratios Sr/Ca and Sr/Ca + K increase for a time, though in the most acid rock of the series which we have been able to examine, both these ratios have lower values than their maximum.

Yttrium. Yttrium increases in amount to some extent as the value of the function $[(\frac{1}{3}\text{Si} + \text{K}) - (\text{Ca} + \text{Mg})]$ becomes greater, and the Y/Ca ratio increases regularly in the same direction.

Lanthanum. Lanthanum is below its limit of sensitivity at the basic end of the series but, like Y, is concentrated to some extent in the later-stage members.

Sodium (*Fig.* 28*g*). Sodium does not vary greatly in amount but reaches a feeble maximum in the middle of the series.

Potassium, Barium, Rubidium, Caesium, Lead (*Fig.* 28*g*). Potassium rises steadily as the value of the function $[(\frac{1}{3}\text{Si} + \text{K}) - (\text{Ca} + \text{Mg})]$ increases. Barium is high throughout and reaches a maximum in the middle of the series. The ratio Ba/K does not vary much except in the most acid specimen which we investigated, where it declines. The curve for rubidium is, as usual, practically parallel with that of potassium throughout the range we covered with our specimens. Caesium

lies below the limit of sensitivity, except in the most acid specimen of those we examined. Lead occurs in small amounts in most of the rocks and increases as the rocks become more acid.

Zirconium (*Fig.* 29). Zirconium rises steadily in amount as the function $[(\frac{1}{3}\mathrm{Si} + \mathrm{K}) - (\mathrm{Ca} + \mathrm{Mg})]$ increases in value. It may, or may not, decline in the extreme late-stage rocks which we have not been able to examine.

Certain olivine basalts of the East Central Sierra Nevada appear to be closely related to the rocks of the latite series, and could well represent accumulative phases of this series. Three examples are given in Table 17 (cols. 7, 8 and 9). Column 10 of the same table shows the trace element content of a basalt which Halsey believes may represent the ultimate parent from which the parental magmas of both the calc-alkali series and the latite series were derived.

The parental magmas

The approximate compositions of the supposed parental magmas, on a water-free basis, of the various rock series dealt with in this paper are collected together in Table 17, with one or two other analyses for comparison. It must be noted that the rocks used in obtaining the composition of the parental magma for the Scottish Tertiary Series were somewhat altered and, moreover, analytical data for the basalts of this series are still very scanty. A relatively low potash content seems to be a general feature of these basalts, and the difference in potash content between the supposed parent of the Scottish Tertiary series and those of the Hawaiian and Polynesian series is probably real.

The analyses in the first eight columns of Table 17 all have a marked family resemblance in spite of differences in Fe/Mg ratio and of minor differences in their contents of alkalis and lime. When plotted to show the variation between magnesium, total iron and total alkalis (Fig. 30), they lie on a smooth curve except for No. 1 (which, as already mentioned, is based on somewhat altered rocks and scanty material) and for No. 5 (which is on the phonolitic line of descent). There is, however, less regularity of behaviour with respect to their contents of calcium, sodium and potassium. We have not enough data on rocks representing these supposed parental magmas to see if there is any systematic variation in trace element behaviour as the Fe/Mg ratio increases (but see p. 277).

Not only are all these analyses similar but they are quite different in character from the parental magmas of the calc-alkali igneous rock series (compare Table 17 here with Table 8 in Nockolds and Allen, 1953, p. 139, and Fig. 30 here with Fig. 15 of that paper). This, of course, is only what we should expect. The supposed parent of the E. Central Sierra Nevada latite series (Table 17, col. 9, and Fig. 30) is different from all the rest and is closely related to parental magmas of calc-alkali type. This is in harmony with the environment and the mineralogy of this latite series.

Acknowledgments We wish to thank Prof. K. C. Dunham, Dr. J. H. Halsey, Mme. E. Jérémine, Dr. G. A. Macdonald, Prof. J. Orcel, Dr. D. B. Slemmons, and Dr. H. Winchell for providing us with samples of rocks which had already been analysed for their major constituents.

References

Bailey, E. B., *et al.* (1924) Tertiary and post-tertiary geology of Mull (Mem. Geol. Surv.), 25–28, 136–145, 185–194

Bandy, M. C. (1937) Bull. Geol. Soc. Amer. **48,** 1596

Campbell, R., Day, T. C., and Stenhouse, A. G. (1933) Trans. Edin. Geol. Soc. **12,** 342–375; **13,** 148–172

Edwards, A. B. (1941) Proç. Roy. Soc. Victoria **53,** 403–415

Harker, A. (1904) Tertiary igneous rocks of Skye (Mem. Geol. Surv.), 256–269

(1908) Geology of the small isles of Inverness-shire (Mem. Geol. Surv.)

Higazy, R. A. (1952) Trans. Edin. Geol. Soc. **15,** 150–186

Lacroix, A. (1927) Mem. Acad. Sci., Paris **59,** 1–82

(1928) C.R. Acad. Sci., Paris **187,** 367–368

(1931) C.R. Acad. Sci., Paris **192,** 1161–1166

(1936a) Le Volcan Actif de L'Ile de la Réunion, Paris, 197–251

(1936b) C.R. Acad. Sci., Paris **202,** 601–604

(1936c) C.R. Acad. Sci., Paris **202,** 788–791

Macdonald, G. A. (1949a) U.S. Geol. Surv., Prof. Paper **214**-D, 51–96

(1949b) Bull. Geol. Soc. America **60,** 1541–1596

Macdonald, G. A., and Powers, H. A. (1946) Bull. Geol. Soc. Amer. **57,** 115–124

Nockolds, S. R., and Allen, R. (1953) Geochim. et Cosmochim. Acta **4,** 105–142

Tilley, C. E. (1950) Quart. J. Geol. Soc. **106,** 37–61

(1952) Amer. J. Sci., Bowen Volume, 529–545

Tomkeieff, S. I. (1937) Bull. Volcan., Ser. 2 **1,** 59–87

Tyrrell, G. W. (1928) Geology of Arran (Mem. Geol. Surv.), 111–122, 236–237, 251

Wager, L. R., and Mitchell, R. L. (1953) Geochim. et Cosmochim. Acta **3,** 217–223

Winchell, H. (1947) Bull. Geol. Soc. Amer. **58,** 1–48

Geochimica et Cosmochimica Acta, 1954, Vol. 5, pp. 286 to 298. Pergamon Press Ltd., London

The origin of native sulphur deposits from isotope fractionation studies*

H. G. Thode, R. K. Wanless† and R. Wallouch‡
Department of Chemistry, Hamilton College, McMaster University, Hamilton, Ontario

(*Received* 27 *January* 1954)

ABSTRACT

Sulphur and carbon isotope abundance studies have been made on the sulphur well cores and adjacent formations of the Texas and Louisiana salt domes. The free sulphur was found to be depleted in S^{34} with respect to associated sulphate by 3·9 per cent on the average. This compares to a 3·2 per cent fractionation of the sulphur isotopes in the formation of free sulphur from sulphate by bacterial action in North African lakes. Also, the associated sulphate was found to be enriched in S^{34} as compared to adjacent anhydrite formations to various extents depending on the sulphur well investigated.

Carbon isotope ratios obtained for the calcite matrix of the sulphur well cores showed that the carbon of the calcite was depleted by from 3·3 to 5·5 per cent in C^{13} as compared to standard limestone. These results indicate that the calcite was formed simultaneously with the free sulphur from carbon of organic origin by a process resulting in some further fractionation of the carbon isotopes.

All the isotope abundance data can be reconciled with the conclusion that the large sulphur deposits of the southwestern United States have been formed by living organisms.

Introduction

Previous investigations have shown wide variations in the abundances of the sulphur isotopes in terrestrial sulphur (Thode *et al.*, 1949; Trafimov, 1949; Thode, 1949; Tudge and Thode, 1950; Thode *et al.*, 1953). In general, it is found that sulphates are enriched and sulphides of sedimentary origin are depleted in S^{34}. Tudge and Thode (1950) have calculated isotopic exchange constants for a number of isotopic reactions involving sulphur and have shown that extensive fractionation of the sulphur isotopes can be expected in biological and geological processes. For example, the exchange constant for the reaction

$$H_2S^{34} + S^{32}O_4^{=} \rightleftharpoons H_2S^{32} + S^{34}O_4^{=} \qquad (1)$$

is 1·074 at 25°C favouring S^{34} in the sulphate. It is apparent that biological and geological processes involving the reduction of sulphate and the oxidation of hydrogen sulphide will tend to establish the most favoured distribution of the sulphur isotopes according to reaction (1). The biological sulphur cycle in the sea illustrated in Fig. 1 is such a process. Previous isotope fractionation studies (Szabo *et al.*, 1950; Thode *et al.*, 1951) show that this cyclic process results in the enrichment of S^{34} in sulphate and in its depletion in free sulphur and sulphide.

Native sulphur is an important intermediate in the sulphur cycle and it is well known that sulphur is formed in the muds at the bottom of lakes and seas by the bacterial reduction of sulphate to hydrogen sulphide and finally by bacterial oxidation to free sulphur. Previous results have shown (Macnamara and Thode, 1951) that sulphur formed in this way was considerably depleted in S^{34} as compared to the source sulphate. It is likely that many of our large sulphur deposits were produced by bacterial action and should show a similar isotope fractionation.

* Presented at annual meeting Geological Society of America, Toronto, Canada, November 9, 10, 11, 1953.

† Now with Radioactive Resources Division, Geological Survey of Canada, Ottawa, Ontario.

‡ Now at North American Cyanamid Laboratories, Niagara Falls, Ontario.

With this in mind, sulphur and carbon isotopic abundance studies were carried out on core samples from Texas and Louisiana sulphur wells.

In these wells native sulphur is found in a matrix of calcitic limestone which usually lies between a layer of anhydrite and gypsum, all of which form the cap rock of salt domes. Louisiana salt domes have been known since 1863. However, these domes excited little interest until the discovery of oil at Spindle Top Dome in 1901. Since then, much has been written concerning the origin of the salt domes

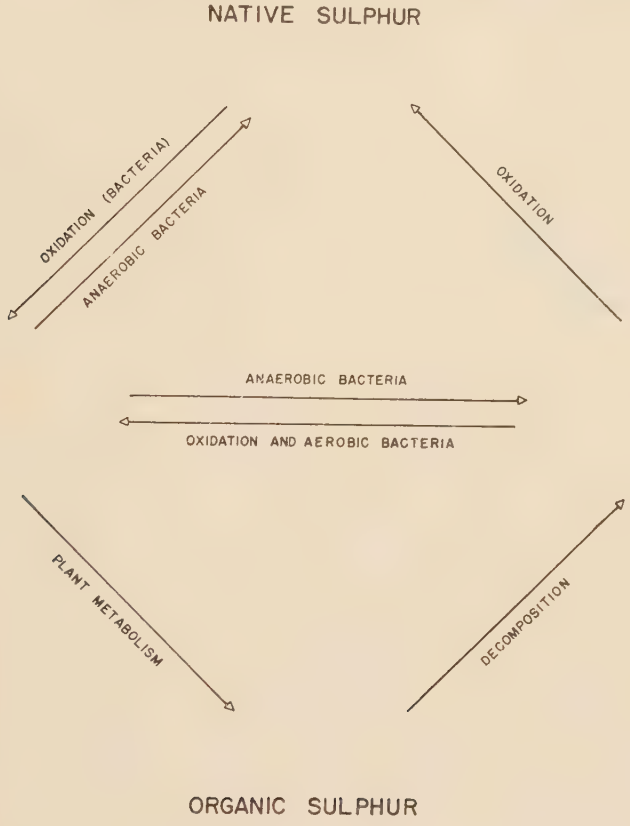

Fig. 1. Biological sulphur cycle.

and the origin of the cap rocks which include the native sulphur deposits (American Association of Petroleum Geologists, 1926; Brown, 1931; Rogers, 1918; Hanna and Wolf, 1934; Marx, 1936). These salt domes are considered to be offshoots of bedded salt deposits formed and forced upwards by pressure in pleistocene times. Fig. 2 illustrates a typical salt dome. The anhydrite cap is of normal marine crystallization and is thought by some to have been forced up ahead of the salt. Whereas, the calcite and gypsum are thought to have been formed by direct alteration of the anhydrite by the action of carbonate waters and water respectively (Brown, 1931). The native sulphur, found in small quantities in a few, is considered to be secondary in origin, having been formed distinctly later than the associated rock.

The Hoskins mound salt dome in Texas is roughly circular and approximately 500 acres in extent (Marx, 1936). The transition from anhydrite to calcitic limestone in this dome is not so pronounced, and in some places the anhydrite has been replaced by calcium carbonate and free sulphur. Unlike the calcitic limestone layer, the anhydrite and gypsum layers are low in porosity. Small amounts of calcite and free sulphur occur in the anhydrite, but these amounts decrease rapidly with depth into the anhydrite. It is interesting to note that all salt domes found with commercial deposits of sulphur have thick layers of the porous calcitic limestone (Lilley, 1936).

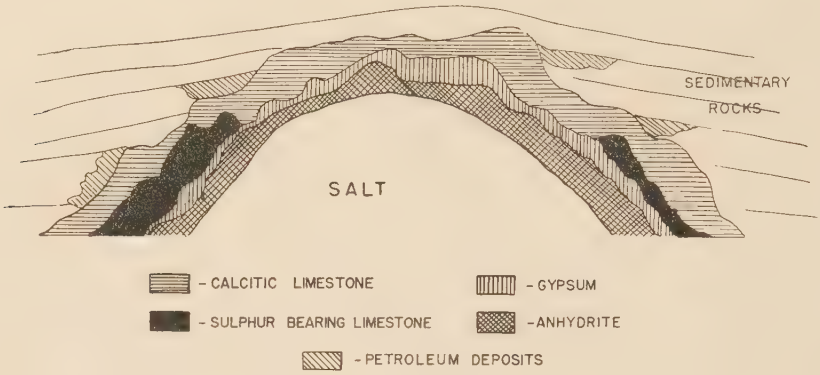

Fig. 2. A typical salt dome.

Since the native sulphur is closely associated with sulphate (anhydrite and gypsum), it has been generally assumed that the sulphur was in some way formed from the sulphate by a reduction process, although hydrogen sulphide gas has also been considered as a possible source of the sulphur. In the case of the sulphate reduction process, two possibilities have been discussed from time to time, first, the reduction of sulphate by organic matter, and second, the reduction of sulphate by bacterial action. The latter reduction process has seemed the most likely, as organic reduction would involve high temperatures and there is no geological evidence for these high temperatures. Nevertheless, evidence for bacterial reduction has also been lacking. It was felt that the sulphur isotopic fractionation studies would provide this evidence and give clues concerning the source and relationship of the anhydrite, gypsum, limestone and sulphur of the salt dome cap rocks.

Experimental

Preparation of sulphur dioxide samples

The core samples investigated contained for the most part large quantities of free sulphur in a matrix of porous calcite with various quantities of sulphate as anhydrite and gypsum and much smaller quantities of sulphide. In the preparation of sulphur dioxide from these three forms of sulphur, procedures were designed to give high yields (greater than 98 per cent) in order to avoid fractionation of the sulphur isotopes.

Free sulphur. Several crystals of free sulphur were selected and crushed to small pieces.

A representative sample of about 25 -50 mg was then burned in a stream of oxygen. The sulphur dioxide formed was frozen in a liquid air trap and later transferred to a standard sample tube after the reaction was complete and after excess oxygen had been pumped off. Using acetone dry ice bath, about 2 per cent of the gas was fractionated off to remove carbon dioxide contamination. Experiments showed that the fractionation of the isotopes which occurred in this procedure was negligible.

Sulphide. A 200–300 gram specimen was crushed to small pieces approximately 0·5 grams in weight. In this state a large part of the free sulphur could be separated out of the sample. The sample was then treated with concentrated hydrochloric acid for three hours. The hydrogen sulphide liberated was carried out by a stream of nitrogen gas into solutions of cadmium acetate. The precipitated cadmium sulphide was later converted to silver sulphide as the latter precipitate was more amenable to washing procedures and could be burned completely to sulphur dioxide in a stream of pure oxygen. The sulphur dioxide produced was collected and treated as described above.

Sulphate. After the three-hour digestion with concentrated hydrochloric acid and the complete removal of hydrogen sulphide, the solution was boiled further for twenty minutes, diluted to three times its volume and filtered. Barium sulphate was then precipitated from the filtrate by the addition of barium chloride according to a procedure prescribed for solutions with high salt concentrations (Warren and Thode, unpublished). The barium sulphate produced was then reduced by magnesium powder in a closed iron crucible in an atmosphere of nitrogen. The procedure involved placing 0·2–0·5 gm of barium sulphate in the iron crucible with three grams of magnesium powder, one gram of the powder being placed below and 2 grams above the sample. Nitrogen gas was passed into the crucible through a ceramic tube leading into the crucible cover. The crucible was heated for 20 minutes at 400°C and then at 650°C for 5 minutes. In this way, the sulphate was reduced to sulphide and the unreacted magnesium converted to magnesium nitride. After cooling the crucible, the porous mass was transferred to an apparatus in which the material could be treated with concentrated hydrochloric acid and the liberated hydrogen sulphide carried in a stream of nitrogen into solutions of cadmium acetate. Again the cadmium sulphide precipitate was converted to silver sulphide by treatment with silver nitrate solution and the washed and dried silver sulphide precipitate was then burned in a stream of pure oxygen and the sulphur dioxide sample prepared as before.

Preparation of carbon dioxide samples

A small sample of the calcitic limestone containing free sulphur was digested with hydrochloric acid and the carbon dioxide liberated was swept into a solution of barium hydroxide in a stream of nitrogen. The barium carbonate precipitate was filtered in a nitrogen atmosphere and dried. About 0·1 gram of this barium carbonate was then completely reacted with concentrated sulphuric acid in an evacuated system and the liberated carbon dioxide was frozen into a pyrex sample tube for removal to the mass spectrometer.

Mass spectrometry

Sulphur isotope ratios were determined with a 90 degree mass spectrometer designed to collect the two ion beams from $S^{32}O^{16}O^{16}$ and $S^{34}O^{16}O^{16}$ simultaneously (Wanless and Thode, 1953; McKinney *et al.*, 1950). A magnetic valve system was employed to permit the rapid comparison of the unknown sample with a standard SO_2 sample prepared from meteoritic sulphur (Beenham, Union County, New Mexico) and arbitrarily assigned an S^{32}/S^{34} ratio of 22·200. It has been possible to reproduce the ratios reported here to within $\pm 0{\cdot}02\%$ from day to day.

The carbon isotope ratios were determined with a 180 degree direction focusing mass spectrometer employing single ion collection. A barium carbonate sample from the laboratory of F. E. Wickman was used as a standard. The isotopic content of this sample has been determined by Harmon Craig and found to be about one per cent light in C^{13} as compared to his standard limestone (Craig, 1953; Craig, private communication). The results reported in Table 6 have been ratioed to Harmon Craig's standard limestone which has a C^{12}/C^{13} ratio of 88·89.

Results and Discussion

Sulphur isotopes

Nine samples of free sulphur were selected from a single sulphur well core about 8 in. long and 3 in. in diameter and the S^{32}/S^{34} ratio determined for each. The results are given in Table 1. The first seven samples were analyzed with a single ion collection instrument and the ratios obtained were reproducible to $\pm 0{\cdot}1$ per cent. The ratios for the last two samples were obtained by a simultaneous collection method with a relative accuracy of $\pm 0{\cdot}02$ per cent. It is clear from these results that the S^{34} content of the free sulphur in a single core is not uniform but varies by from 0·1 to 0·5 per cent. The sulphur isotope abundance data obtained with a relative precision of $\pm 0{\cdot}02$ per cent for the sulphate, free sulphur and sulphide present in eleven different sulphur well core samples taken from ten different salt domes is given in Table 2. In each case, the sulphur dioxide used for analysis was prepared from a representative sample obtained from 200–300 grams of core rock. Columns 7 and 8 give the S^{34} enrichment factors comparing sulphate with free sulphur and sulphide respectively. These factors show that the free sulphur is depleted in S^{34} with respect to the associated sulphate by 3·9 per cent on the average, and that the sulphide is depleted still further in this isotope by about 1·0 per cent.

Table 1. Sulphur isotope ratio variations within core No. 10, Spindletop Dome Sulphur Well

Sample No.	S^{32}/S^{34} *Sulphur*
0	22·14 ± 0·02
1	22·05 ± 0·02
2	22·14 ± 0·02
3	22·10 ± 0·02
4	22·15 ± 0·02
5	22·13 ± 0·02
6a	22·17 ± 0·02
6b	22·10 ± 0·02
7	22·153 ± 0·004*
8	22·199 ± 0·004*

* Samples 7 and 8 were analyzed using simultaneous collection methods—the others with single collection on 180° mass spectrometer.

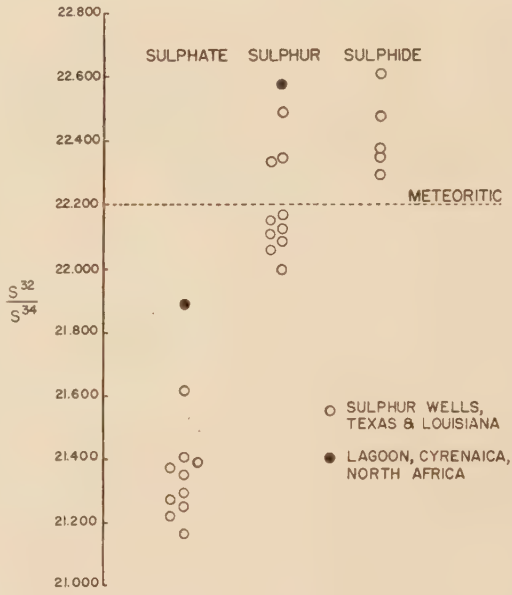

Fig. 3. S^{34} variation found in sulphur, sulphate and sulphide from sulphur wells of Louisiana and Texas.

The isotopic ratios for the sulphate, free sulphur and sulphide given in Table 2, columns 4, 5 and 6, are plotted in Fig. 3 to show the spread in values from one sulphur well to another for each form of sulphur. The S^{32}/S^{34} ratio is seen to vary

over a considerable range, the spread amounting to 2·25 per cent for both sulphate and free sulphur and to an overall spread of 6·2 per cent between the lowest ratio for sulphate to the highest for sulphur.

Finally, in Table 3 the sulphur isotope abundance data obtained for the adjacent anhydrite, gypsum and salt formations of the Long Point dome in Texas are compared with the corresponding data of the sulphur-bearing limestone. The sulphate with the highest enrichment of S^{34} is seen to occur in the calcitic

Table 2. Sulphur isotope abundance data for Texas and Louisiana sulphur wells

Core No.	*Location*	*Depth (in feet)*	S^{32}/S^{34}*			*Enrichment factor*	
			$SO_4^=$ R1	S^0 R2	$S^=$ R3	$S^0/SO_4^=$ R2/R1	$S^=/SO_4^=$ R3/R1
6	Moss Bluff Dome, Liberty Co., Texas	885	21·404	22·344	22·472	1·044	1·050
4	Piedras Pintas Dome, Duval Co., Texas	550	21·395	22·166	22·376	1·036	1·046
7	Boling Dome, Wharton Co., Texas	704	21·613	22·127	22·341	1·024	1·034
5	Long Point Dome, Ft. Bend Co., Texas	718	21·395	22·341	22·341	1·044	1·044
9	Orchard Dome, Ft. Bend Co., Texas	767	21·297	22·488	22·609	1·056	1·062
2	Clemens Dome, Brazoria Co., Texas	1109	21·224	21·997		1·036	
10	Spindletop Dome—1	1492	21·272	22·119		1·040	
10	Spindletop Dome—2	1492	21·354	22·153		1·037	
3	Starks Dome, Calcasieu Parish, Louisiana	1521	21·377	22·080	22·297	1·033	1·043
8	Lake Washington, Plaquenimes Parish, Louisiana	1553	21·164	21·997		1·039	
1	Hoskins Mound, Brazoria Co., Texas	1860	21·259	22·056		1·037	
			Average			1·039	1·047

* All ratios obtained with a precision of ±0·02 per cent.

limestone layer which contains the free sulphur. The gypsum and anhydrite formations which in this particular salt dome occur above and below the limestone bed respectively show little evidence of sulphur isotope fractionation. Their S^{32}/S^{34} ratios are higher and in the range of values found for sea water sulphate (21·750 to 21·850) (Warren and Thode, unpublished). The salt sulphate

Table 3. Sulphur isotope abundance data, Jefferson Lake Sulphur Co. Well No. 142, Davis Long Point Dome, Fort Bend County, Texas

Sample	Formation	Depth (in feet)	S^{32}/S^{34}			Enrichment factor	
			$SO_4^=$ R1	S^0 R2	$S^=$ R3	$S^0/SO_4^=$ R2/R1	$S^=/SO_4^=$ R3/R1
1	Gypsum ($CaSO_4.2H_2O$)	833	21·758	22·193	22·302	1·020	1·025
2	Calcitic-sulphur bearing Limestone	958	21·533	22·198	22·366	1·031	1·039
3	Anhydrite ($CaSO_4$)	965	21·858		22·277		1·019
4	Salt	981	22·012				
5	No. 5 Core, Long Point Dome, Fort Bend Co.	718	21·395	22·341	22·341	1·044	1·044

which is further removed from the sulphur-bearing limestone is found to have a still higher S^{32}/S^{34} ratio. These results indicate that the reduction of sulphate to free sulphur and sulphide has taken place locally and that adjacent layers of sulphate have not been involved to any great extent.

Bacterial reduction of sulphate. The results of Table 2 show that the S^{34} enrichment factor between sulphate and free sulphur is remarkably constant, the average value being 1·039. This result is even more remarkable when the large spread in isotopic ratios from one well to another is considered (see Fig. 3). It seems clear, therefore, that the sulphur has been formed from the associated sulphate by a low temperature reduction process which results in a considerable fractionation of the sulphur isotopes. Previous work in this laboratory (Thode *et al.*, 1951) has shown that in controlled laboratory experiments using a pure culture of Vibrio desulphuricans, the common sulphate-reducing bacteria, the hydrogen sulphide produced in the sulphate-reduction process is depleted in S^{34} by about 1 per cent at 25°C. It has been found more recently that this fractionation of the sulphur isotopes is increased at lower temperatures (2 per cent at 10°C) (Wallouch *et al.*, unpublished). Also Feely, Gast and Kulp (1953), have confirmed fractionation factors of this order of magnitude. These laboratory experiments carried out under controlled conditions show that where free sulphur is formed by the bacterial reduction of sulphate, sulphur isotope fractionation can

be expected in the same direction as that found for the sulphur wells, but perhaps not of the same magnitude. However, when hydrogen sulphide and free sulphur are formed by bacterial reduction of sulphate in natural environments, fractionation factors of the order reported in Table 2 for the sulphur wells are found.

In the sulphur-producing lakes of North Africa, a layer of free sulphur is deposited each year, formed by the reduction of sulphate due to the action of the reducing bacteria Vibrio desulphuricans. Table 4 shows the isotope fractionation

Table 4. Isotope fractionation in bacterial reduction of native sulphur from sulphate

Sample	S^{32}/S^{34}		*Enrichment factor* $S^0/SO_4^=$
	$SO_4^=$	S^0	
Native sulphur*		22·57	1·032
sulphate*	21·88		
Average sea water sulphate	21·80		

* Native sulphur and sulphate from lagoon in Cyrenaica, North Africa.

factor found by Macnamara and Thode (1951), between free sulphur and associated sulphate in these lakes. It is seen that sulphur isotope fractionation is in the same direction and of the same order of magnitude (values actually overlapping), as that found for the Texas and Louisiana sulphur wells, Table 2. Also, water from wells and sulphur springs in Southern Ontario is known to contain reducing bacteria which produce hydrogen sulphide from the sulphate in the water. Table 5 shows the sulphur isotope fractionation factors between sulphate and hydrogen sulphide in those waters, reported by Thode *et al.* (1949). Although there is a considerable spread in values, the average fractionation factor of 1·033 is again close to the 1·047 value found for the sulphur wells under investigation.

The laboratory reduction experiments were carried out under quite different conditions from those which occur in nature and therefore the lack of agreement in the magnitude of the isotope effects is not surprising. For example, in the reduction of sulphate to hydrogen sulphide and then to sulphur (oxidation) in a natural environment a considerable amount of sulphur may be lost as hydrogen sulphide gas. In the sulphur-forming lakes in North Africa hydrogen sulphide is evolved at all times (Butlin, 1953). Also, hydrogen sulphide seepage from salt domes is common. Actually in the absence of photo-synthetic bacteria and other oxodizing processes reduction of sulphate can take place without the formation of free sulphur. This situation may have prevailed to a large extent in the case of salt domes with a layer of calcitic limestone but with little or no evidence of free sulphur.

In the case of the sulphur-producing lakes in North Africa, the sulphate was found to have a S^{32}/S^{34} ratio very close to that of sea water sulphate, indicating a

large reservoir of sulphate with little evidence of overall S^{34} enrichment. The enrichment factor of 1·032 found between sulphate and free sulphur may therefore represent a close approach to the fractionation factor for the natural lake process. However, in the case of the salt domes, the residual sulphate samples associated with the free sulphur in the cap rock show various degrees of enrichment in S^{34} from one sulphur well to another (see Table 2). This enrichment has undoubtedly come about because a large fraction of the sulphate in a localized region, probably

Table 5. Comparison of isotope abundance data for $SO_4^=$ and H_2S present together in well water from different locations

Location	S^{32}/S^{34}		*Enrichment factor* $S^=/SO_4^=$
	$SO_4^=$	$S^=$	
Dorcester, Ont.	21·735	22·705	1·045
Tillsonburg, Ont.	21·715	22·180	1·021
Port Ryerse, Ont.	21·650	22·400	1·035
Port Stanley, Ont.	21·585	22·215	1·029
	Average		1·033

in solution, has been reduced to hydrogen sulphide and free sulphur. Since these later compounds are depleted in S^{34}, the residual sulphate becomes richer and richer in this isotope as the reaction proceeds. Because of this "batch process" concentration of S^{34} in the residual sulphate, the simple isotope separation factor of the salt dome reduction process is difficult to establish. In general, the average isotope enrichment factor (1·039) reported in Table 2 will be higher than the simple separation factor since the isotopic ratio S^{32}/S^{34} of the residual sulphate is compared with that of the total free sulphur produced.

An accurate calculation of the separation factor from the isotope data of Table 2 is not possible since the S^{34} enrichment in the residual sulphate will depend on many unknown factors such as the initial sulphate concentration, the fraction of sulphate reduced, the degree of mixing of sulphate during the process and the fraction and isotopic concentration of reduced sulphur lost from the system as hydrogen sulphide. However, a comparison of the S^{32}/S^{34} ratio of the free sulphur with that of the adjacent anhydrite cap rock (initial sulphate) should give the lower limit of the separation factor. The average separation factor calculated in this way assuming the S^{32}/S^{34} ratio of the initial sulphate to be 21·80, which is both an average for sea water sulphate and for the adjacent gypsum and anhydrite formations (Table 3), is 1·017. The separation factor for the salt dome process must therefore be between 1·017 and 1·039.

It should be pointed out that there is little correlation between the enrichment factors found for the sulphur wells and the degree of enrichment of S^{34} in residual sulphate, although core sample No. 7 with the least S^{34} enrichment in the sulphate does show the smallest enrichment factor. A considerable loss of hydrogen sulphide before the free sulphur began to form could lead to enrichment of S^{34} in the sulphate without any effect on the enrichment factor found between residual sulphate and free sulphur formed near the end of the process.

So far there has been little attempt to simulate nature in the laboratory experiments involving the bacterial reduction of sulphate. In these later experiments, the hydrogen sulphide produced by a pure strain of Vibrio desulphuricans in a sterile nutrient was swept out by a stream of nitrogen and its isotopic content compared with that of the sulphate medium. The low fractionation factors found at 25°C (1·01) indicates that isotopic equilibrium between sulphate and hydrogen sulphide according to reaction (1) is certainly not attained. Further, unpublished work in this laboratory (Wallouch *et al.*, unpublished) suggests that the isotope fractionation for this rapid enzyme catalyzed reduction process occurs in the initial step, namely in the reduction of sulphate to sulphite and involves perhaps both a kinetic and equilibrium isotope effect.

In sulphur-producing lakes, and in all natural environments, all kinds of anaerobic and aerobic bacteria are present and both oxidation and reduction processes are involved. Near the lake bottoms conditions will be right for the anaerobic processes and sulphate reduction can be expected to occur. Whereas, in the aerated layers near the surface the aerobic bacteria will predominate and oxidation of sulphur and hydrogen sulphide to sulphate will take place. These processes taken together form a sulphur cycle. Under these conditions there may very well be a trend toward isotopic equilibrium between sulphate and hydrogen sulphide (reaction 1). This, of course, would mean a much higher enrichment factor on the average between sulphate and free sulphur. Experiments are now in progress to simulate this natural process in the laboratory.

Carbon isotopes

In the bacterial reduction of sulphate some reducing agent such as lactate or other organic matter is necessary to provide a source of free energy. Sulphate is reduced to hydrogen sulphide and free sulphur and the organic matter is oxidized to carbon dioxide and water. In this regard petroleum is often associated with salt domes and there is considerable evidence of organic matter in the core samples themselves. Such a process in the anhydrite cap rock of the salt domes should result in some free sulphur in a matrix of calcitic limestone. This is essentially the kind of formation found over most salt domes. Actually, only those salt domes with thick layers of calcite have commercial deposits of sulphur (Lilley, 1936). If the calcite is formed in this way, then the carbon in the calcite will be of organic origin, and have a low C^{13} content (Craig, 1953). With this in mind, the carbon isotopes of the calcitic cores were investigated.

In each case, the isotopic ratio of the calcitic core sample was compared with that of a standard limestone. The results are given in Table 6. Column 4. The C^{13} content of the calcite in the sulphur well cores is seen to be depleted in C^{13}

by from 3·3 to 5·5 per cent as compared to standard limestone. This is certainly definite proof that the cap rock calcite was not deposited as limestone at the bottom of a shallow sea in equilibrium with sea water carbonate.

Using the C^{12}/C^{13} ratio found for limestone as standard, Craig (1953) has shown that terrestrial plants, coal and petroleum are depleted in C^{13} by about 3 per cent. It is seen that some of the calcite samples show an even greater depletion in C^{13} and, in fact, have the lowest C^{13} content of any terrestrial carbon reported to date.

Table 6. Carbon isotope abundance data for Texas and Louisiana sulphur wells

Core No.	*Location*	*Depth (in feet)*	$\frac{C^{12}/C^{13}}{C^{12}/C^{13}*}$	$\frac{S^{32}/S^{34}}{S^0/SO_4^=}$
10	Spindletop Dome—1	1492	1·055	1·040
10	Spindletop Dome—2	1492	1·049	1·037
3	Starks Dome, Calcasieu Parish, Louisiana	1521	1·048	1·033
1	Hoskins Mound, Brazoria County, Texas	1860	1·047	1·037
7	Boling Dome, Wharton County, Texas	704	1·037	1·024
6	Moss Bluff Dome, Liberty County, Texas	885	1·033	1·044

* Compared to limestone with $C^{12}/C^{13} = 88·89$ (Craig, 1953; Craig, Private communication).

Certainly the results substantiate the view that the calcitic carbon in the salt dome sulphur wells is of organic origin, a situation which would prevail if the native sulphur were formed by living organisms from sulphate and organic reducing agents.

The extra depletion in C^{13} over that of organic matter could be explained by a further fractionation of the carbon isotopes in the oxidation of the organic matter due to kinetic effects. Carbon dioxide produced in decarboxylation reactions for example is usually depleted in C^{13} by about 1–3 per cent (Lindsay *et al.*, 1951; Bigeleisen, 1949).

The variations in isotopic ratios both for the carbon and sulphur isotopes within a single core sample are also indicative of the kind of localized process one would expect if living organisms were responsible for the formation of free sulphur and calcite in the salt dome cap rock.

Conclusions

The sulphur and carbon isotope fractionation studies add greatly to our knowledge of the origin of free sulphur deposits in the cap rock of salt domes and point definitely to living organisms as the responsible agents. Vibrio desulphuricans, the sulphate-reducing bacteria, are found almost everywhere in springs, wells and in the sea. Observations made on artesian well waters near Tripoli show the sulphate reducers are active in the earth to a depth of 1,200 metres at temperatures of

63°C and at considerable pressures (Butlin, 1953). Certainly the reducing bacteria are present in the sulphur wells of Louisiana and Texas. The sulphur and carbon isotope abundance data for these wells taken together provide overwhelming evidence that the native sulphur was formed by these living organisms. The main factors may be listed as follows:

(1) The S^{34} enrichment factor between free sulphur and associated sulphate is large and remarkably constant for the sulphur well cores of Louisiana and Texas.

(2) The average enrichment factor of 1·039 compares with 1·032 found in the case of the sulphur-producing lakes of Africa where bacterial reduction of sulphate is known to take place.

(3) The large enrichment factor and the S^{34} enrichment found for the residual sulphate in the sulphur-bearing cores indicate a localized low temperature reduction process.

(4) The lack of isotopic uniformity within the sulphur or sulphate of a single core sample is not a common phenomenon and suggests a localized reduction process in the cap rock with a large isotope effect.

(5) The very low C^{13} content of the sulphur-bearing calcitic limestone indicates that the calcite was formed from carbon of organic origin.

(6) The lack of carbon isotope uniformity in the calcite again points to a localized production of calcite.

The correlation between the sulphur and carbon isotope data is perhaps the strongest evidence in favour of the bacterial reduction process since this process would involve the reduction of sulphate to hydrogen sulphide and the simultaneous oxidation of organic matter to carbon dioxide. All the isotope abundance data can be reconciled with the conclusion that the large sulphur deposits in the south-western United States have been formed by means of living organisms.

References

Rogers, G. S. (1918) Intrusive origin of Gulf Coast salt domes. Economic Geology **13,** 447

American Association of Petroleum Geologists (1926) Geology of salt dome oil fields, 3 volumes

Brown, Levi S. (1931) Cap rock petrography. Bull. Amer. Assoc. of Petrol. Geologists **15,** 509

Hanna, M. A., and Wolf, A. G. (1934) Texas and Louisiana salt dome cap rock minerals. Bull. Amer. Assoc. of Petrol. Geologists **18,** 212

Lilley, E. R. (1936) Economic geology of mineral deposits. Henry Holt and Co., New York, 640

Marx, Archer H. (1936) Hoskins Mound salt dome, Brazoria County, Texas. Amer. Assoc. of Petrol. Geologists **20,** 170

Bigeleisen, J. (1949) Isotope effect in the decarboxylation of labelled malonic acids. J. Chem. Phys. **17,** 425

Thode, H. G. (1949) Variations in abundances of isotopes in nature. Research **2,** 154

Thode, H. G., Macnamara, J., and Collins, C. B. (1949) Natural variations in the isotopic content of sulphur and their significance. Can. J. Research **B27,** 361

Trafimov, A. (1949) Isotopic composition of sulphur in meteorites and terrestrial objects. Doklady Akad. Nauk. S.S.S.R. **66,** 181

McKinney, C. R., McCrea, J. M., Epstein, S., Allen, H. A., and Urey, H. C. (1950) Improvements in mass spectrometers for the measurement of small differences in isotope abundance ratios. Rev. Sci. Inst. **21,** 724

Szabo, A., Tudge, A., Macnamara, J., and Thode, H. G. (1950) The determination of S^{34} in nature and the sulphur cycle. Science **3,** 464

Tudge, A. P., and Thode, H. G. (1950) Thermodynamic properties of isotopic compounds of sulphur. Can. J. Research **B28,** 567

Lindsay, J. G., Bourns, A. N., and Thode, H. G. (1951) C^{13} isotope effect in decarboxylation of normal malonic acid. Can. J. Chem. **29,** 192

Macnamara, J., and Thode, H. G. (1951) The distribution of S^{34} in nature and the origin of native sulphur deposits. Research **4,** 582

Thode, H. G., Kleerekoper, H., and McElcheran, D. (1951) Isotope fractionation in the bacterial reduction of sulphate. Research **4,** 581

Butlin, K. R. (1953) The bacterial sulphur cycle. Research **6,** 184

Craig, H. (1953) The geochemistry of the stable carbon isotopes. Geochim. et Cosmochim. Acta **3,** 53

Craig, H. (1953) Private communication

Feely, H. W., Gast, P. W., and Kulp, J. L. (1953) Abundance of S^{32} and S^{34} in some natural sources of sulphur. Geological Society of America Annual Meeting, Toronto, Canada, 55

Thode, H. G., Macnamara, J., and Fleming, W. H. (1953) Sulphur isotope fractionation in nature and geological and biological time scales. Geochim. et Cosmochim. Acta **3,** 235

Wallouch, R., Wanless, R. K., Warren, J., Kleerekoper, H., and Thode, H. G. (1953) Unpublished work in this laboratory

Wanless, R. K., and Thode, H. G. (1953) A mass spectrometer for high precision isotope ratio determinations. J. Sci. Inst. **30,** 395

Warren, J., and Thode, H. G. (1953) Unpublished work in this laboratory

GEOCHEMICAL NOTE

Meteorites in the Carl Bosch Collection of Minerals Yale University

(*Received* 22 *March* 1954)

The purpose of this communication is to call attention to a large collection of meteorites which has not been previously described. The fact that meteorite collections are extremely slow in growth testifies to the significance of the sudden appearance of one such as this. This preliminary note anticipates a complete catalogue now in preparation.

There are more than 600 meteorites, representing more than 300 falls, in the Carl Bosch Collection of Minerals. This collection, comprising more than 25,000 specimens, was deposited in the Peabody Museum of Natural History of Yale University in 1949. It was accumulated by CARL BOSCH, Sr., of Berlin, Germany, and was brought to the United States by his son, CARL BOSCH, Jr., in 1949.

The falls represented in the collection have all been described previously. Twenty-six falls are represented by samples weighing less than one gram; 51 samples weigh between 1 and 10 g; 105, 10–100 g; 75, 100–500 g; 18, 500–1000 g; and 20 weigh more than 1000 g. Three very large masses weigh more than 100 pounds: Gibeon, Great Namaqualand, South-West Africa (100 pounds *ca.*), a mass of 432 pounds, and a mass of 573 pounds. Specimens totalling more than 500 grams include:

Admire, Lyon County, Kansas, U.S.A.	559 g
Arispe, Sonora, Mexico	610
Bischtübe, Nikolaev, Turgai, Siberia	1722
Bjurböle, Borgå, Nyland, Finland	1190
Bluff, Fayette County, Texas, U.S.A.	1109
Brenham Township, Kiowa County, Kansas, U.S.A.	686
Cañon Diablo, Coconino County, Arizona, U.S.A.	3367
Chupaderos, Jimenez, Chihuahua, Mexico	2375
Coahuila, Mexico	603
Covert, Osborne County, Kansas, U.S.A.	1365
Ergheo, Brava, Italian Somaliland, East Africa	559
Fisher, Polk County, Minnesota, U.S.A.	736
Forest City, Winnebago County, Iowa, U.S.A.	1173
Forsyth County, North Carolina, U.S.A.	638
Gibeon, Great Namaqualand, South-West Africa	5900*
Gilgoin Station, Brewarrina, County Clyde, New South Wales	2122
Henbury, McDonnell Ranges, Central Australia	1180
Imilac, Desert of Atacama, Chile	18,630
Kenton County, Kentucky, U.S.A.	612
Locust Grove, Henry County, Georgia, U.S.A.	2011
McKinney, Collin County, Texas, U.S.A.	1439
Mocs, Cluj, Transylvania	1010
Mount Dyrring, Singleton district, County Durham, New South Wales	509

* In addition to the large mass described *supra*.

N'Goureyma, Jenne, Massina, French West Africa	544g
Oakley, Logan County, Kansas, U.S.A.	1171
Olivenza, Badajoz, Spain	576
Pultusk, Warsaw, Poland	1011
Roebourne, North-West Division, Western Australia	580
Sacramento Mountains, Eddy County, New Mexico, U.S.A.	704
San Angelo, Tom Green County, Texas, U.S.A.	921
San Cristobal, Antofagasta, Chile	500
Santa Catharina, Brazil	618
São Julião de Moreira, Ponte de Lima, Minho, Portugal	1796
Tennasilm, Esthonia, Baltic States	3825
Toluca, Mexico State, Mexico	6234
Vaca Muerta, Taltal, Atacama, Chile	641
Vigarano, Ferrara, Italy	1442
Youndegin, Avon, South-West Division, Western Australia	858

In addition there is a large slab of the Tocopilla meteorite weighing several pounds. There are 33 tektites, 5 pseudometeorites, some telluric irons, and some dust. Complete data including the types and weights will be published in the *Postilla* series of the Peabody Museum together with a revised list of the meteorites in the Peabody Museum Collection.

KURT SERVOS

Department of Geology
Yale University
New Haven, Conn.

Announcement

CLAY MINERAL TECHNOLOGY

is the theme of the Third National Clay Minerals Conference to be held at the Rice Institute, Houston, Texas, October 27–28–29, 1954. The Conference is sponsored by the Clay Minerals Committee of the National Research Council. A special part of the programme will be devoted to fundamental or applied papers. Anyone interested in presenting papers in *any* of these or *other* fields pertaining to clays or related minerals is invited to announce their intentions to A. F. FREDERICKSON, Washington University, St. Louis 5, Missouri, on or before July 15, 1954.

A detailed programme, including field-trip information, will be available on request in August, 1954. *Everyone* interested in any aspect of clay mineralogy, technology or related fields is cordially invited to attend the Conference.

INFORMATION FOR CONTRIBUTORS

I. GENERAL

1. Papers on Geochemistry should be submitted to the editors for the appropriate country or language (*Papers on Cosmochemistry should be sent to Prof. F. A. Paneth, F.R.S.*). Papers submitted for publication will naturally be judged from the standpoint of scientific originality and novelty. Technical details of apparatus used in scientific investigation can, however, be presented in brief notes. The preparation of progress reports and review articles will be invited by the Editors from time to time. The Journal will appear as independent and complete numbers, which will be sold separately and combined into volumes of about 300 pages.

2. Only papers which have not been previously published will be accepted. The publishers retain exclusive publication rights for all papers in all languages and countries, on acceptance and until the 31st December of the year following the year when the printed paper appears. Authors must agree not to publish elsewhere a paper submitted to and accepted by *Geochimica et Cosmochimica Acta.*

3. Authors will receive 75 free reprints of their papers. Additional copies can be purchased if ordered at the time the first proofs are returned.

II. MANUSCRIPT REQUIREMENTS

1. The manuscript must be written in one of the three official languages, English, French, or German.

2. The manuscript should be an original typewritten copy (not a carbon). The text must be ready for printing and should be carefully checked for errors. Authors will receive proofs for correction.

3. Half-tone illustrations are to be restricted to the minimum necessary. They should accompany the manuscript mounted on separate sheets. Line drawings may be redrawn for the sake of uniformity and should therefore include all relevant details. Photographs should be enlarged sufficiently to permit their clear reproduction in half-tone. If words or numbers appear in photographs, two copies are requested, one clearly printed and the other without inscription. All illustrations should be provided with descriptive legends, which should accompany the manuscript on a separate sheet.

4. Only such references to literature should be given as are referred to in the text. Literature references are to be listed together at the end of the manuscript and not given as footnotes. **All references should be listed alphabetically according to the Harvard system :**

AHRENS, L. H. (1952) Geochim. et Cosmochim. Acta, 2, 168.

and should include the standard abbreviated title of the journal, year, volume number and page number.

5. The text of articles submitted should be concise and in a readily understandable style. The technical description of the methods used should only be given in detail when such methods are new. The essential contents of each paper should be briefly recapitulated in an abstract in English. Such an abstract may, however, be submitted by the author in the language of the original typescript for translation into English by the editorial staff.

6. To conserve space authors are requested to mark less important portions of the paper (such as description of methods, record of experimental results, etc.) for printing in smaller type.

PERGAMON PRESS LTD

Books of interest to readers of this journal

READY SHORTLY

COALS AND BITUMENS and related fossil carbonaceous substances

By S. I. TOMKEIEFF, D.Sc. *About 17s. 6d. net*

This book (the first of its kind) contains a glossary of terms relating to fossil carbonaceous substances, mainly coals and bitumens. The terms are arranged in two parts:

(*a*) An alphabetical glossary in which each term is concisely defined, giving, when possible, an etymological definition and references.

(*b*) Synoptic tables in which the terms are arranged in natural groups and sub-groups.

Among the terms are names of varieties of coals and bitumens, both scientific and vernacular, names relating to the petrography of coal and names relating to oil shales and other carbonaceous material. A list of most common German and French terms, and some other terms, is appended. The Introduction contains a simple and rational classification of fossil carbonaceous substances. Impartial, concise and easy to handle, this book is unique in the respect that the glossary covers a large number of terms relating to a restricted branch of science. *Crown 8vo. 128 pages.*

QUANTITATIVE SPECTROCHEMICAL ANALYSIS OF SILICATES

By L. H. AHRENS, D.Sc., F.R.I.C. *About 25s. net*

A very useful book for the geochemist, describing for the first time a scheme of quantitative D.C. arc spectrochemical analysis of the naturally occurring silicates (minerals, rocks, meteorites and coils), which attempts to reach an effective compromise between speed, sensitivity and cost of analysis. *Demy 8vo. About 120 pages. Well illustrated.*

IN PREPARATION

ISOTOPE GEOLOGY

By KALERVO RANKAMA, Ph.D. *About 70s. net*

Cooperation between nuclear physics and geology has produced results pertaining to the history, structure, and chemical composition of the Earth and its heat balance. Both sciences have profited from this cooperation.

This book is divided into two parts. Part I tries to give, for a geological reader, an account of the physics and chemistry of nuclides and of the principal methods used in research in isotope geology. Part II deals with the natural science of nuclides, i.e., their manner of occurrence in Nature. It is a collection of data and an attempt at its explanation. *Large Royal. About 500 pages.*

Prices quoted are British prices only

242 MARYLEBONE ROAD · LONDON N·W·1

PRINTED AT THE PITMAN PRESS, BELFAST